SUNY College of Environmental Science and Forestry

Digital Commons @ ESF

Dissertations and Theses

Winter 11-20-2020

Modeling Heat Exchange of White-Tailed Deer (Odocoileus Virginianus) In the Built and Natural Environments of Fire Island, New York

Kaitlyn Fox
SUNY College of Environmental Science and Forestry, kfox1619@gmail.com

Follow this and additional works at: https://digitalcommons.esf.edu/etds

Part of the Environmental Monitoring Commons

Recommended Citation

MODELING HEAT EXCHANGE OF WHITE-TAILED DEER (*ODOCOILEUS*

VIRGINIANUS) IN THE BUILT AND NATURAL ENVIRONMENTS OF

FIRE ISLAND, NEW YORK

by

Kaitlyn E. Fox

A thesis
submitted in partial fulfillment
of the requirements for the
Master of Science Degree
State University of New York
College of Environmental Science and Forestry
Syracuse, New York
November 2020

Department of Environmental and Forest Biology

Approved by:
H. Brian Underwood, Major Professor
Robert W. Malmsheimer, Chair, Examining Committee
Melissa K. Fierke, Department Chair
S. Scott Shannon, Dean, The Graduate School

ACKNOWLEDGEMENTS

TABLE OF CONTENTS

LIST OF TABLES

LIST OF FIGURES

LIST OF APPENDICES

ABSTRACT

K. E. Fox. Modeling Heat Exchange of White-tailed Deer (*Odocoileus virginianus*) in the Built and Natural Environments of Fire Island, New York, 84 pages, 5 tables, 11 figures, 2 appendices, 2020. Ecology style guide used.

The potential consequences of climate warming on the behavior and distribution of endotherms pose management challenges. This is especially true for organisms that are able to exploit both natural and anthropogenic environments, such as the white-tailed deer. I developed a biophysical model of operative temperature based on various forms of heat transfer between deer and their environment on Fire Island National Seashore using measured variables collected from a small micrometeorological sensor network. I compared operative temperature to observed values of Vernon globe temperature in order to validate the use of the globe as a representation of heat exchange for deer. The globe was an adequate proxy, with minimal difference between the predicted and observed values and compatibility in patterns over the diel. Identifying critical thermal thresholds for deer in a changing landscape will be necessary in order to understand and address future human-wildlife interactions.

Keywords: climate change, Fire Island National Seashore, heat transfer, operative temperature, thermal environment, Vernon globe temperature, white-tailed deer

K. E. Fox
Candidate for the degree of Master of Science, November 2020
H. Brian Underwood, Ph.D.
Department of Environmental and Forest Biology
State University of New York College of Environmental Science and Forestry,
Syracuse, New York

PROLOGUE

Climate change poses numerous threats to biodiversity worldwide. A projected increase in temperature of anywhere from 3 °C to 6 °C is expected in the Northeast United States by the 2080s if global emissions continue to escalate (Horton et al. 2014). In addition to sea level rise and greater vulnerability to hurricanes, the frequency and intensity of heat waves is expected to increase, which will likely cause shifts in species distribution and migration of land-cover types (Kearney et al. 2009a, Horton et al. 2014, Fuller et al. 2016). While noticeable differences will be seen in ectotherms, thermoregulatory responses in endotherms may not be as obvious, as they maintain a constant core body temperature by managing heat gain and loss through morphological, physiological and behavioral mechanisms (Porter and Gates 1969, Hetem et al. 2007, Kearney and Porter 2009). Although energy imbalances experienced over shorter time scales may not be as meaningful, long-term inequities will have deleterious consequences (Bunnell et al. 1986, Johnston and Schmitz 1997). These consequences are especially true for species with a single birth pulse per year, such as white-tailed deer (*Odocoileus virginianus*), where homeostasis over the annual cycle is critical for survival, successful reproduction and offspring care.

One of the important questions surrounding deer and other temperate zone ungulates is how they will respond and compensate to maintain thermal balance when the climate becomes unsuitable to the point where they can no longer dissipate heat adequately (Porter and Kearney 2009, Melin et al. 2014). Evaluation of the utility, availability and variability of thermal cover, food and fresh water, as well as the relationship and trade-offs between these factors, is necessary in order to predict the needs of this species and how their activity and utilization of space will change over time (Johnston and Schmitz 1997, Mysterud and Østbye 1999, Büntgen et

al. 2017). For instance, during the summer, large temperate herbivores trade-off between forage availability and thermal cover – browsing in open habitats and resting in forested areas – but they can be tolerant of thermal stress when high quality food is available (Mysterud and Østbye 1999, Massé and Côté 2013). The results of analyses on the relationship between an organism and its thermal environment can provide insight into the potential consequences of climate warming on deer distribution and potential future conflicts in human-dominated landscapes. However, many models that examine movement, distribution and behavior focus on those species adapted for specific thermal regimes that are moving to the edge of their range boundaries (e.g., moose [Alces alces] in New York at their southern range for the species in North America), and few have addressed these factors simultaneously at varying temporal scales (Saupe et al. 2011, Massé and Côté 2013, Elmore et al. 2017). Additionally, little attention has been given to species that exploit both natural and anthropogenic environments, particularly when anthropogenic environments may provide thermoregulatory benefits that afford them with a better opportunity to maintain homeostasis (Walker 2006).

The purpose of this thesis is to develop a model of operative temperature (T_e), a biophysical computation of energy balance based on the theorized relationship of heat transfer between an organism and its environment. This was done in order to validate the use of the 127-mm Vernon globe as a proxy of heat exchange for white-tailed deer on Fire Island National Seashore, NY, a coastal barrier system comprised of both natural and anthropogenic habitat, and to conceptually visualize the thermal environment of deer. In this document, I explain the construction and execution of the model and present comparisons of T_e and Vernon globe temperature.

LITERATURE REVIEW

Organismal Thermal Balance

The interaction between an organism and its thermal environment is dependent on multiple heat transfer processes (Moen 1973, Campbell and Norman 1998). Convection, conduction, evaporation and radiation are the primary methods responsible for the gain or dissipation of heat, and as a result, alterations in body temperature, metabolic heat production or evaporative cooling are required to maintain homeostasis (Bakken et al. 1985, Norris and Kunz 2012). The rate and degree of heat gained from the environment and heat lost to the environment is controlled by properties possessed by the animal, such as the surface area in contact with radiation, the presence or absence of a coat or feathers (external insulation), pelage thickness and condition (e.g., wet or dry), peripheral blood flow, body size and shape, orientation, posture and color, among others (Walsberg 1992, Fuller et al. 2016). In addition, environmental conditions such as the form of solar radiation (i.e., short wave or long wave), fractional absorptivity and irradiance, surrounding vegetation and soil layers, cloud cover, humidity and solar elevation angle must be considered when addressing the complex physiological and biological process that determine the overall temperature of an organism in its habitat (Moen 1973, Bakken 1976, Bakken 1992). Understanding and quantifying the heat load on an animal is necessary to determine current status of and future changes to life history, demography, behavior and intra- and interspecific interactions as a result of climate change (Huey 1991).

Climate Change and Thermal Balance

Over the last century, temperatures in the northeastern United States have increased by about 1 °C above pre-industrial levels (Horton et al. 2014). The potential impacts of 1.5 °C and 2°C global warming were recently outlined by the Intergovernmental Panel on Climate Change

(IPCC), and projections for the next several decades indicate that more frequent and intense heat waves, increases in precipitation, and a rise in sea levels that are expected to exceed the global average of 0.3 to 1.2 m by 2100 are likely (Horton et al. 2014, IPCC 2018).

A primary question concerning endotherms' behavioral response to rising temperatures, therefore, is where they will go if their current habitat becomes unsuitable (Long et al. 2014, Thaker et al. 2019). Büntgen et al. (2017) analyzed hunting/harvesting locations of the four most abundant ungulate species in the European Alps – ibex (*Capra ibex*), chamois (*Rupicapra rupicapra*), red deer (*Cervus elaphus*), and roe deer (*Capreolus capreolus*) from 1991 to 2013. Interannual and decadal increases in average hunting elevation were a result of autumnal warming, with drastic changes seen among ibex, chamois and red deer, and moderate changes among roe deer, likely due to the latter's preference for meadows in valley bottoms during autumn and winter. Changes in energy balance over time affect fitness, so behaviors that buffer an animal against negative environmental variation should be favored (Long et al. 2014). Consequently, it is important to understand how the trade-offs required to achieve homeostasis in the face of climate warming affect behavior, distribution, and therefore predation, parasitism, competition and disease dynamics (Huey 1991, Huey et al. 2012).

Although endotherms are able to internally regulate their body temperature, exposure to significant heat gain can cause damage to temperature-dependent enzymes necessary for metabolism, impeding survival and reproduction (Norris and Kunz 2012). Additionally, large endotherms are more likely to overheat due to smaller surface area to volume ratios and thick boundary layers (the pelage barrier, or hair-air interface, between the skin and the surrounding atmosphere) that prevent heat from escaping into the environment (Porter and Gates 1969, Moen 1973). Sufficient energy is required to maintain homeostasis, so in extreme environments, the

sole use of metabolic processes can be inadequate in stabilizing core body temperatures (Hetem et al. 2010, Norris and Kunz 2012). For this reason, endotherms have adopted a wide range of physiological and behavioral mechanisms in order to thermoregulate, such as placing themselves in open areas exposed to wind, seeking thermal cover, or positioning their bodies in a way that will increase or decrease the amount of direct solar radiation they intercept (Mysterud and Østbye 1999, Melin et al. 2014, Wiemers et al. 2014). The Arabian oryx (*Oryx leucoryx*) of Saudi Arabia employed adaptive heterothermy, whereby body heat was stored during the day and dissipated non-evaporatively during the night in order to conserve body water (Hetem et al. 2010). Another mammal living in similar shade-free conditions, the black wildebeest (*Connochaetes gnou*), altered its posture, orientation and feeding time to maintain its core body temperature, which changed depending on the availability of water (Maloney et al. 2005). Ungulates occupying colder regions that are susceptible to warm temperatures such as moose (*Alces alces*) sought out areas with higher and denser canopy cover in order to dissipate and avoid gaining heat (Melin et al. 2014).

In addition to altering the surrounding thermal environment, climate change also indirectly changes composition, location or quality of forage (Fuller et al. 2016). Wiemers et al. (2014) discovered that male white-tailed deer in southern Texas did not trade off selection of food for thermal cover, but instead sought cooler environments and higher forage quality during midday in order to maintain energy balance. A combination of taller vegetation, woody plant canopy cover and cooler T_e provided the best explanation for habitat selection during this time. In a similar study, Long et al. (2014) modeled the spatio-temporal trade-offs that North American elk (*Cervus elaphus*) face between reducing thermoregulatory costs and searching for high quality forage in two contrasting ecosystems – a high-elevation desert and a temperate,

montane forest. Elk in the desert chose areas that reduced thermoregulatory costs over those with high quality forage, whereas those in the forest did the opposite.

Understanding the varying levels of vulnerability that different species will face in the wake of climate change predictions is a necessity in order to develop effective management plans (Kearney et al. 2009a, Huey et al. 2012). While these species may currently have the means to alleviate the consequences of heat stresses, there is a great deal of uncertainty facing them as global temperatures continue to rise and their existing habitats become less suitable (Fuller et al. 2016). Many large terrestrial mammals face increased risk of extinction in the wake of climate change due to life history traits such as the late age of sexual maturity, long gestation periods and low number of offspring per year, necessitating the identification of thermal refuges and settings with extreme thermal conditions that pose significant risk to survival and reproduction (Long et al. 2014, Fuller et al. 2016, Elmore et al. 2017). While adapting to increases in temperature and scarcities of food and water will be difficult, larger mammals can move faster and have lower energy costs related to body mass compared to smaller mammals, which may allow them to relocate to more suitable habitats, especially if the novel habitats are connected to currently occupied ranges (Fuller et al. 2016).

Microclimate Models

Many species distribution models (SDMs) and ecological niche models (ENMs) have been designed to examine the current and future impacts of climate warming on the spatio-temporal range boundaries and ecological niche of organisms with greater accuracy. A combination of energy and mass balance equations, geographic distribution data and environmental predictor variables are connected to computer-generated algorithms that can be projected on current and future landscapes to forecast species' responses to changing conditions.

Moose, deer, spiders and toads are only a few examples of organisms that have been assessed using these models (Bartelt et al. 2010, Saupe et al. 2011, Melin et al. 2014, Dawe and Boutin 2016).

Bartelt et al. (2010) modeled the movements and patterns of habitat use of Western toads (*Anaxyrus boreas*) in Idaho by evaluating the landscape's topography, climate and vegetation, as well as the animal's physiology and behavior. Climate change may limit toad activity due to the increased physiological costs (such as evaporation tolerance) associated with landscapes as global temperatures continue to rise. Saupe et al. (2011) investigated the current and prospective future distribution of the venomous brown recluse spider (*Loxosceles reclusa*) throughout the eastern half of the United States using the Genetic Algorithm for Rule-set Prediction and Maxent concluding that the spider is likely to extend northward into previously unoccupied territory based on two emission scenarios from IPCC3, one liberal (the A2 scenario) and the other conservative (the B2 scenario). Melin et al. (2014) assessed the structure and location of vegetation in relation to moose behavior in Finland under different thermal conditions using global positioning system collar data and airborne laser scanning. While moose actively sought out higher and denser canopies when temperatures exceeded 20 °C, indicating an advantageous behavioral shift during periods of extreme heat, they will still be severely impacted by climate warming. Dawe and Boutin (2016) used an SDM to predict prospective white-tailed deer range expansion in Canada and determined that less severe winters and longer growing seasons as a result of climate change would increase the likelihood of deer presence.

However, despite extensive study of a wide range of organisms, these models are often focused on species at their range boundaries, where responses to a hostile environment (or conditions outside the zone of least metabolic effort) are likely to be observed first (Bartelt et al.

2010, Saupe et al. 2011, Melin et al. 2014, Dawe and Boutin 2016). Although species that are near their range boundaries will not be excluded from the potentially deleterious effects of climate-warming on thermal balance, they will instead show more nuanced responses in their overall thermal balance over space and time (Kearney and Porter 2009). Additionally, many spatial and temporal field studies do not have the capacity to gather sufficient information on real-world systems due to the wide spatial range of many larger species, such as ungulates (Johnston and Schmitz 1997, Maloney et al. 2005).

In order to develop more robust predictions about these types of responses, there is a growing need to incorporate organisms' physiological dimensions and thermal limitations as a function of climate into distribution models (Kearney and Porter 2009, Porter et al. 2010, Thaker et al. 2019). Boldrini et al. (2018) modified one classical model predicated on the assumption that conduction and convection were the only modes of heat transfer inside and outside an organism's body, respectively. Their model incorporated four layers; the body core, the tissues surrounding the body core, the tissue near the surface which transfers heat via conduction, and the coat layer, which interacts with the external ambient temperature via convection, evaporation and radiation. By accounting for several dynamic mechanisms of thermoregulation in endotherms, this approach may further the understanding of how heat transfer in various parts of the body interact with one another and help develop more accurate and realistic models of thermal balance.

Additionally, there are challenges involved with converting information on broad climatic shifts to local scales to determine the direct impacts on individual organisms (Kearney et al. 2009b). Many animal-climate response models take a correlative approach, whereby spatial data is statistically connected to records of species distribution (Kearney and Porter 2009). While

useful for species that have not been well-studied, this approach may be difficult for range-shifting species because it requires projecting results from intricate statistical models onto novel, unsampled spaces, and does not account for the organism's underlying physiological constraints, potentially leading to inaccurate predictions (Kearney et al. 2008, Kearney and Porter 2009). Instead, there is a need for an approach that is independent of the known geographic range of a species and focuses on treating an organism not as a static data point, but as a being composed of morphological, physiological and behavioral traits (Kearney et al. 2009a, Kearney and Porter 2009).

Efforts to address these issues may involve a mechanistic approach where biophysical models are constructed in a climate-space using morphological, physiological and behavioral restraints of a specific species together with spatial data on climate, topography, vegetation and measurements of microclimatic conditions (Porter et al. 2010). The climate-space takes into account both the absorbed radiation and air temperature in which the subject can survive and designates upper and lower limits of extremes that gauge the suitability of the surrounding environment (Porter and Gates 1969, Johnston and Schmitz 1997, Sharpe and Van Horne 1999). A notable advantage of this type of model is that it incorporates a realistic level of complexity that allows for a more accurate connection between the surrounding ambient temperature and the body temperature of the organism. Ultimately, the mechanistic model can isolate organism traits that will hinder the species' response to changes in climate as well as the processes required for survival and reproduction (Kearney and Porter 2009, Kearney et al. 2009b).

Vernon Globe Temperature

One index that estimates the combined effect of abiotic elements of an animal's microclimate is Vernon globe temperature (Panagakis 2011). First introduced in the 1930s,

Vernon's globe thermometer was originally intended to measure human comfort levels by simultaneously evaluating the effects of solar radiation, wind velocity and air temperature (Kuehn et al. 1970, Hetem et al. 2007). The results were based on the assumption that unequal air and radiant temperature could be physiologically equal – an assumption that had been called into question but could not be accurately tested until the development of a costly and intricate environmental chamber (Wenzel and Forsthoff 1989). Using men running on treadmills, Wenzel and Forsthoff (1989) determined that constant globe temperatures returned varying physiological responses and the construction of a modified globe that simulated the flow of heat in the human body was necessary in order to reflect the decreased heart rates and rectal temperatures in the men associated with increasing radiant temperatures and decreasing air temperatures.

One such measure to achieve a better simulation of heat flow was to reduce the diameter of the globe, thereby increasing the convective heat transfer coefficient, a step taken in studies of other mammals such as free-ranging ungulates (Hetem et al. 2007), dairy ewes (*Ovis aries*; Panagakis 2011) and goats (*Capra aegagrus hircus*; Maia et al. 2014, 2016). Hetem et al. (2007) fit 0.030 m diameter mini-globe thermometers to collars on blue wildebeests (*Connochaetes taurinus*), impalas (*Aepyceros melampus*) and horses (*Equus caballus*) which revealed that wildebeests tended to seek sites that protected them from the wind, while horses and impalas chose sites that provided protection from the sun. Panagakis (2011) used a 0.038 m diameter globe to examine the relationship between Vernon globe temperature and heat stress of dairy ewes in hot environments, concluding that their minimum and maximum respiratory rates were correlated with that of Vernon globe temperatures and that they sought shade during the day and cooled off at night. Using a globe with a diameter of 0.15 m, Maia et al. (2014) determined that goats with black and white coats in Brazil require shade as protection from solar radiation levels

above 800 Wm^{-2}, as they increase metabolic heat production when exposed to higher levels.

Ultimately, Vernon globe temperature can more accurately depict the way an animal experiences its thermal environment than ambient temperature because the apparatus fully absorbs incoming solar radiation (Elmore et al. 2017). Additionally, Vernon globes have been used in conjunction with other meteorological variables in order to circumvent costly and cumbersome taxidermic mounts of the animal and can act as a surrogate for a calculated temperature index, operative temperature (T_e), that incorporates many elements of heat exchange between an animal and its environment (Hetem et al. 2007, Wiemers et al. 2014, Elmore et al. 2017).

Operative Temperature

In order to assess the conditions of surrounding microhabitats, measurements of T_e have been used to indicate an animal's body temperature at thermal equilibrium in the absence of metabolic heating and evaporative cooling (Bakken et al. 1985, Dzialowski 2005). This metric is defined as the temperature of an isothermal blackbody enclosure with the same heat transfer mechanisms as the actual environment, and incorporates solar radiation, air temperature and wind speed on a spatio-temporal scale (Bakken et al. 1985, Campbell and Norman 1998). First introduced by Winslow et al. (1937) with relation to humans, T_e is a physiological approach that incorporates environmental heat transfer processes as well as thermoregulatory and morphological characteristics of the study animal. The results have been used for a wide range of applications including thermal mapping, assigning thermal values and habitat suitability indices to animals' home ranges, as well as determining the energetic costs of particular environments for amphibians, insects, birds, reptiles and mammals (Bakken 1976, Dzialowski 2005, Huey et al. 2012).

Reports of ambient temperatures were once considered to be adequate when describing the way an animal felt in its environment; however, over time it became clear that it was necessary to incorporate components of the animal's physiology, morphology and biogeography and account for the effects of other environmental factors such as solar radiation and wind speed to obtain a more accurate depiction of the thermal environment, opening the door for measurements like T_e (Elmore et al. 2017). Many past models of T_e were created to estimate the potential body temperature of ectotherms (Bakken 1992, Kearney and Porter 2009, Huey et al. 2012), but have since been used for large mammals such as mule deer (*Odocoileus hemionus*) and cattle (Parker and Gillingham 1990, Beaver et al. 1996, Turnpenny 1997). Two fundamental approaches involved constructing hollow body mounts and placing them around the organism's habitat to measure T_e, or collecting microclimate measurements and integrating those data with morphological properties of the animal such as size, shape and color to create mathematical models that calculate T_e (Huey 1991, O'Connor and Spotila 1992). The first approach requires the use of a heated or unheated thermal mount of the animal that was either composed of copper and covered with the animal's pelt or feathers to correct for resistance to absorption, materials with the same resistance as the animal, or the carcass of the animal (Bakken et al. 1985, Bakken 1992). While useful for obtaining instant estimates of T_e, building thermal mounts is time-consuming and costly, and there are limited inferences that can be made regarding heat transfer dynamics due in part to their immobility (Huey 1991, Bakken 1992).

Although older models used simple mathematical equations to calculate T_e, computer-generated 3D models using thermal imaging, deterministic mathematical equations and environmental simulation programs have become more common (Beaver et al. 1996, Dzialowski 2005). These models allow for predictions of T_e under increasingly complex and accurate

environmental conditions, including hypotheticals, and include physiological and morphological

properties of the animal (Huey 1991, Sharpe and Van Horne 1999, Wiemers et al. 2014).

Operative temperature also incorporates elements that cause thermal stress (e.g., solar radiation

and wind speed) omitted from other indices such as the thermoneutral zone and incorporates

measurements taken from the field as opposed to those simulated in a laboratory (Fuller et al.

2016).

All biophysical models ultimately rest on a series of tenuous assumptions and empirical

approximations such that simplifications are often necessary when presented with a lack of

information on the animal or the complexity of interactions being described. Consequently,

beginning with a simple model and expanding upon it is advised (Moen 1973, O'Connor and

Spotila 1992). Errors among replicate studies and the lack of calibration for many models of T_e

are additional problems that must be addressed (Dzialowski 2005).

INTRODUCTION

The influence of the thermal environment on organismal heat balance has been examined

in multiple domesticated and wild, free-ranging species (Parker and Gillingham 1990, Beaver et

al. 1996, Sharpe and Van Horne 1999, Maloney et al. 2005, Hetem et al. 2010, Panagakis 2011,

Long et al. 2014, Maia et al. 2014, Wiemers et al. 2014, Maia et al. 2016). In order to address

questions about species' impending movement, distribution and behavior, a variety of

biophysical models of mass and energy balance have been constructed. Parker and Gillingham

(1990) modeled critical thermal environment thresholds for mule deer that accounted for various

wind speeds, air temperatures and solar radiation levels. Beaver et al. (1996) used a Vernon

globe thermometer and resistance to heat loss from micrometeorological data collected in

Montana to successfully predict standard operative temperature (T_{es}; heat flow between a

controlled laboratory and the natural environment) for mule deer and cattle. Sharpe and Van Horne (1999) revealed that Piute ground squirrels (*Spermophilus mollis*) in southwestern Idaho were not active during midday by examining how movement patterns were linked to varying thermal conditions. Maloney et al. (2005) observed thermoregulatory behaviors and activity patterns of black wildebeest in South Africa and found the species favored night feeding and standing when ambient temperatures were high. Hetem et al. (2010) determined that irregularities in body temperature of Arabian oryx in Saudi Arabia were due to changes in ambient temperature and water availability. Panagakis (2011) revealed the link between respiration rates of lactating dairy ewes and Vernon globe temperature in Greece, as ewes sought shade during the heat of the day and cooled off at night. Maia et al. (2016) determined that goats in Brazil dissipated heat via cutaneous evaporation and respiratory heat loss at air temperatures beyond 30 °C in order to maintain thermal equilibrium.

An organism's response to changes in the thermal environment, however, is difficult to quantify over space and time (Johnston and Schmitz 1997, Huey et al. 2012, Massé and Côté 2013). Despite comprehensive analyses on the costs of thermoregulation and subsequent behavioral and physiological trade-offs, extensive animal movement and the lack of long-term monitoring have made it difficult to define the relationship between range shifts and climate change for many endotherms (Büntgen et al. 2017). Additionally, missing information on the fundamental niche of species (all of the hypothetical combinations of environmental conditions that describe the needs and tolerances of a species) makes predicting their response to changes difficult (Fuller et al. 2016). Besides the variable understanding of how physical changes, such as alterations to vegetation, affect species' tolerance to heat stress, behavior and distribution, the challenges of relating lab-based experiments to conditions in natural heterogenous landscapes

often leaves the influence of temperature on species, particularly endotherms, and their use of habitats out of management plans (Elmore et al. 2017). The selection of cover, for example, either as concealment from predators or thermal refuge, is difficult to discern (Wiemers et al. 2014, Elmore et al. 2017). In order to address how an animal's chosen space compares to the broader environment, determining the scale upon which to examine the question is extremely important; however, many models that have attempted to identify the traits that help species alleviate the effects of climate change have not been met with much success (McCain and King 2014). There is a growing need to develop mechanistic models where a species' physiological, morphological and behavioral constraints are combined with spatial data and measurements of microclimatic conditions and integrated with heat fluxes to predict heat loads and potential activity patterns on organisms (Huey 1991, Porter et al. 2010). Though rising temperatures are commonly portrayed as having negative consequences for endotherms, there may be some animals that can escape, use buffers or possibly benefit from these changes (McCain and King 2014, Büntgen et al. 2017).

White-tailed deer (*Odocoileus virginianus*) are ubiquitous large mammals in the eastern United States with great cultural and economic significance. Understanding the response of this important animal to climate change is vital for long-term planning of everything from recreational harvest to land use. Once on the brink of extinction in 19th century New York due to widespread deforestation and overhunting, after successful introductions in the last four decades white-tailed deer began to outstrip available resources across the state and caused significant ecological and agricultural damage as well as an increase in tick-borne diseases and vehicular collisions (Duffy et al. 1994, Department of Environmental Conservation 2018a). The population of white-tailed deer on Fire Island, adjacent to one the most highly-suburbanized parts of New

York, has been increasing steadily since the establishment of the National Seashore on September 11, 1964 (Underwood 2005). While only 46 deer were documented in 1971, distance sampling conducted from 2016 to 2019 indicated that there were approximately 400 deer across the island, and these numbers have fluctuated between 300 and 700 from surveys dating back to 1989, with a peak of 700 deer in 2003 (NPS 2019b).

Despite the expansion of hunting and culling, public opposition and local ordinances prohibiting the use of firearms in certain areas have made it difficult to implement targeted actions to significantly reduce populations (Underwood 2005, Department of Environmental Conservation 2018b). Changes in human land-use have provided additional support, as deer browse and graze along forest-edge habitats carved out by residential and agricultural development (Department of Environmental Conservation 2018a).

In addition to being generalists able to exploit a wide variety of ecosystems, the complete absence of natural predators on Long Island and Fire Island such as coyotes (*Canis latrans*), wolves (*Canis lupus*), bobcats (*Lynx rufus*), mountain lions (*Puma concolor*) and bears (*Ursus americanus*) have allowed deer populations to flourish (Department of Environmental Conservation 2018b). An average of two fawns per year coupled with this absence of predation have allowed deer to deplete native herbaceous, sapling, and seedling layers, thereby preventing survival to maturity (and thus regeneration), reducing understory plant diversity and creating space for invasive species to outcompete natives (Rawinski 2008, Department of Environmental Conservation 2018b, NPS 2019b). Fire Island presents a unique combination of highly urbanized regions and rare, old-growth vegetation communities that have both been influenced by an overabundance of deer for several decades (Forrester 2004, Forrester et al. 2006).

Despite their success, deer face limitations and potential trade-offs when confronted with adverse climate conditions. Winter, for example, is often marked by decreased activity and weight loss due to scarcities of food and energy costs associated with moving through snow (Dusek et al. 2006). Energy deficits during such seasons cause difficulty in maintaining a high core body temperature, and many endotherms experience reductions in mass of visceral organs and consequently decrease their metabolic rate (Fuller et al. 2016). In addition to undergoing the aforementioned adjustments, red deer also increased the rates of peptide and glucose transport in the small intestines to more efficiently extract nutrients from limited forage in the winter to compensate for changes in plant quality between seasons (Arnold et al. 2015).

While deer face challenges in cold climates, heat presents a different suite of issues. Large mammals tend to regulate core body temperature within relatively narrow limits, possibly giving them greater scope for heat storage; however, excess heat results in reduced forage intake in an effort to moderate metabolic heat production, which over time threatens daily survival and reproduction by disrupting embryonic and fetal development in females and reducing sperm output for males (Norris and Kunz 2012, Fuller et al. 2016). In addition, high temperatures can burden the processes of ruminant digestion by which nutrients are extracted from the already limited forage (Lu 1989), possibly driving deer to alter their behavior so they can locate areas that allow them to break down food without employing costly methods of thermoregulation.

Although range shifts and genetic adaptations are improbable for many species that face human-made obstacles such as roads and extensive settlements, must travel extreme distances, or have already reached the edge of their range, deer on Fire Island may be able to direct energy towards survival and reproduction if they can exploit anthropogenic structures and landscapes to reduce the costs of thermoregulation. Evidence of the ability of deer to thrive among humans on

Fire Island has been well-documented (Underwood 2005, Forrester et al. 2006, Kilheffer et al. 2019), and factors such as the influence of high densities and changes in their movement and behavior (particularly in and around populated human settlements) are and will likely continue to be a primary concern.

In order to assess the conditions of the surrounding environment, measurements of T_e have been used to indicate an animal's body temperature at thermal equilibrium (Bakken et al. 1985, Huey 1991, Bakken 1992). Due to its utility in quantifying the thermal environment, I modeled T_e for deer over space and time using data from a small micrometeorological sensor network. The computation takes into account solar radiation as a function of location, date and time, ambient temperature, wind speed, the thermal constants characteristic of deer and other physical constants. Calculations of T_e have helped determine upper and lower limits of an organism's thermoregulatory capacity within a specific microhabitat and can also be incorporated into maps that display the current thermal environment over space and time (Dzialowski 2005).

The overarching goal of my project is to demonstrate how T_e for deer on Fire Island changes over space and time in order to better understand and assess the potential consequences of climate warming on their behavior and distribution in the built and natural environment. The specific objectives of this study are to: 1) construct a biophysical model of T_e for white-tailed deer based upon established heat transfer principles, and 2) validate the use of the 127-mm Vernon globe thermometer as a T_e proxy for heat exchange in deer by comparing modeled outputs with Vernon globe temperature measured in the field on Fire Island.

STUDY AREA

Fire Island National Seashore (40.703586 N, 72.952014 W) is an approximately 51 km-long, 0.5 km-wide barrier island 24.9 km^2 in size and situated about 6 km south of Long Island, New York (Figure 1). The island includes a variety of terrestrial ecosystems such as primary dunes, shrublands, interdunal swale, beaches, broadleaf forests, a rare, old-growth maritime American holly (*Ilex opaca*) forest (Sunken Forest) and salt and freshwater marshes (Klopfer et al. 2002). Integrated in these ecosystems are 17 private residential communities, two towns, three villages, a county park and the Otis Pike Fire Island High Dune Wilderness Area (OPWA), the only federally designated wilderness area in New York State (Kilheffer 2018). The OPWA is roughly 558-ha and 11-km long and extends from Watch Hill to Smith Point County Park (NPS 2018). The Great South Bay and Moriches Bay separate Fire Island from Long Island.

At least 237 species of plants have been identified across the island, some of the more prevalent being beach grass (*Ammophila breviligulata*), seaside goldenrod (*Solidago sempervirens*), poison ivy (*Toxicodendron radicans*), beach plum (*Prunus maritima*), northern bayberry (*Myrica pensylvanica*), Virginia creeper (*Parthenocissus quinquefolia*), sassafras (*Sassafras albidum*), serviceberry (*Amelanchier canadensis*), red maple (*Acer rubrum*), blackgum (*Nyssa sylvatica*), smooth cordgrass (*Spartina alterniflora*), saltmeadow cordgrass (*Spartina patens*), inland salt grass (*Distichlis spicata*), black cherry (*Prunus serotina*), highbush blueberry (*Vaccinium corymbosum*) and black chokeberry (*Aronia melanocarpa*) (NPS 2019a).

Monthly winter temperatures may reach below -18 °C; late summer months may experience temperatures greater than 38 °C and are usually humid. Average annual temperature is 10.7 °C and a mean annual rainfall is 117 cm (Art 1976, Forrester 2004). Wind speed and direction vary based on season and play a major role in the convective heat transfer of animals

living on the island. Measurements recorded from December 2010 to January 2020 by the Coast Guard Station located near Democrat Point indicated that winds are predominately out of the northwest from December through March and out of the southwest from April through November, with the exception of May where winds were principally out of the southeast. Wind speeds from the prevalent direction ranged from 2 to 12 ms^{-1}, while average speeds throughout the recorded time span did not exceed 1.4 ms^{-1}. The micrometeorological stations deployed to collect this data are typically mounted 1.5 m above the ground on a 3 m instrument tower.

The western half of Fire Island is primarily dominated by residential communities, including houses, restaurants and shops. The eastern half encompasses the OPWA. Between the heavily populated regions and the OPWA are small, scattered green spaces which make up about 30% of the island's natural areas. The OPWA makes up the other 70% (Underwood 2005). Similar to other Atlantic barrier islands, primary dunes run along the ocean and salt marshes line the bay. My research is primarily focused on OPWA and Watch Hill where the micrometeorological stations are located.

The impact of white-tailed deer across Fire Island has presented numerous challenges and uncertainties regarding the management of the island's natural resources, and has required comprehensive investigations into native vegetation conditions, the spread of tick-borne illnesses and human-wildlife interactions. While the exact date that deer colonized the island is unknown, reports of their native presence date back to the turn of the 20th century. Populations have been monitored using aerial and ground surveys since the early 1980s and mid 1990s, respectively, and have grown dramatically since 1983, partially due to the absence of natural predators (Underwood 2005). Herd sizes have fluctuated over time across the island, but some discernable trends have emerged from surveys conducted from the late 1990s to the early 2000s. One survey

in 1991 revealed that while a relatively stable herd was located in the OPWA, the natural zones

and parks to the west were experiencing a 30% increase per year, although there were noticeable

declines from 1994 to 1998 and populations eventually stabilized. Based on monitoring from

1999 to 2005, the average density of deer in the mid-island communities and the OPWA was

estimated to be around 65 deer/km^2 and 25 deer/km^2, respectively. Deer have an average home

range length of 2.4 km, which they occupy to a relatively predictable extent, but it is believed

that populations in the eastern section of the island may have been responsible for the eventual

rapid increase that occurred in the west (Underwood 2005).

METHODS

Data Collection and Organization

In January 2016, ten battery-powered and weatherproof micrometeorological stations

were positioned across Fire Island National Seashore (Table 1). Five of the stations were placed

in OPWA, and five were deployed in Watch Hill (Figure 2), the National Park Service (NPS)

ferry terminal complex that contains a number of houses, boardwalks and other structures

commonly found in the built environment of Fire Island. A base station (Davis VantagePro2

Plus™) was established at the horse corral near the ferry terminal entrance. Each

micrometeorological station was mounted on 1.22-m tall PVC pipes filled with sand; however,

only 0.61 m were exposed above the sand. Every station had an Onset Hobo Micro Station Data

Logger (Onset, Bourne, MA), an Onset 8-bit Temperature Smart Sensor (2-m cable), an Onset

Solar Radiation Shield, an Onset 16-bit Wind Speed Smart Sensor Set and a 127-mm copper

sphere painted matte black. The Vernon globe spheres were placed at the mid-rib height of a deer

(about 51 cm) and the anemometers were placed an additional 30 cm above the spheres.

Vernon globe thermometers were constructed by inserting Onset 12-bit Smart Sensor thermistors into copper spheres (Figure 3). The sphere was designed to mimic the rate of heat exchange between a deer and its environment (Hetem et al. 2007). If convection and radiation coefficients of the sphere mimic those of the animal subject, then the Vernon globe thermometer provides a direct reading of T_e (Kerslake 1972). Each station collected measurements of ambient temperature, Vernon globe temperature and steady and gust wind speeds every 10 minutes. The base station also recorded relative humidity, rainfall, wind direction and solar radiation. Each data logger was equipped with a built-in USB port for data readout. The names of the stations were as follows: Base Station, High Dune, Holly Grove, House, Low Dune, Marsh, Overwash, Phrag, Pine Grove and Swale.

Several trips to replace batteries and read out data were made throughout 2016. The stations were removed during two separate trips in June 2019. Data were downloaded, visualized and extracted using HOBOware™ Graphing and Analysis Software. I organized the data files from each station into separate Microsoft Excel spreadsheets containing the day, month, year and time that each entry of steady wind and gust speeds (ms^{-1}), ambient temperature (°C) and Vernon globe temperature (°C) were recorded. The entries ranged from January 12, 2016 to July 14, 2018. Each station took entries at different time stamps, but all stations registered measurements at the 10-minute intervals. Of the two years of data that were available, the most continuous record occurred for 385 days from January 13, 2016 to January 31, 2017. In order to ensure that all stations had the same record of hours, days, months and years, any corrupted or missing data were replaced with NAs in the spreadsheet. I aggregated the data over each hour resulting in 9,240 entries per station (i.e., 24 hours x 385 days). Hours that did not contain 6 entries of non-missing data were set to NAs prior to analysis.

Micrometeorological Station Locations

The micrometeorological stations were located in a variety of vegetation community types throughout the OPWA and the adjacent built environment of Watch Hill. Stations were distributed from the dune ridge to the marsh, in full, partial and no shade conditions to account for as broad a range of microclimate conditions as possible. The Base Station was located in the center of the circular horse corral near an NPS maintenance and equipment station in Watch Hill. High Dune was positioned on the peak of a dune in OPWA among low-lying herbaceous vegetation such as northern bayberry. Holly Grove was located in a maritime forest in OPWA consisting of American holly, sassafras, serviceberry and other hardwood trees. House was located underneath House 12 – a residential housing unit in Watch Hill used by the NPS. Low Dune was located in Watch Hill on a small dune surrounded by a variety of low-lying herbaceous plants similar to those at High Dune. Marsh was located in a salt marsh in OPWA inundated by water, cordgrasses and saltgrasses. Overwash was located in sand that was deposited from a previous overwash event in OPWA and was surrounded by beach grass. Phrag was positioned in a dense stand of phragmites (*Phragmites australis*) that was inundated with water in Watch Hill. Although no measurements of the height of the phragmites were taken, at the time of retrieval the reeds were several meters above the height of the station. Pine Grove was located in a forest of maritime pitch pine (*Pinus rigida*) and other low-lying herbaceous plants such as poison ivy in OPWA. Swale was located several hundred meters away from a public boardwalk in Watch Hill surrounded by low-lying herbaceous vegetation.

Model of operative temperature, T_e

Multiple investigators (including Bakken and Gates 1975, Bakken 1976, Bakken et al. 1985, Bunnell et al. 1986, Parker and Gillingham 1990, Huey 1991, Bakken 1992, Beaver et al. 1996, Campbell and Norman 1998, Sharpe and Van Horne 1999, Dzialowski 2005, Hetem et al. 2007, Huey et al. 2012 and Wiemers et al. 2014) have outlined and implemented various approaches to calculating T_e. However, the consistent foundation of the metric is based on convective and radiative heat transfer, which is meant to measure the temperature of an animal in thermal equilibrium with its environment in the absence of metabolic heat production and evaporative cooling (Dzialowski 2005). Using heat transfer mechanisms, I created a similar construct of T_e for white-tailed deer which was modeled using the following equation:

$$T_e = T_a + \frac{P_{Sun} - \varepsilon_D \sigma A_D T_a^4}{\frac{K_{fur} A_D}{f_D} + \frac{K_{air} A_D}{\delta_{BL}}}$$

(1)

where T_e is operative temperature (K), T_a is the ambient temperature (K) of the microclimate, P_{Sun} is the absorption rate of solar radiant energy by deer (W), $\varepsilon_D \sigma A_D T_a^4$ is the heat flow rate radiated from deer (W), $\frac{K_{fur} A_D}{f_D}$ is the conduction heat expression (WK^{-1}) and $\frac{K_{air} A_D}{\delta_{BL}}$ is the convection heat expression (WK^{-1}; Table 2, Appendix A).

I developed this equation by identifying the four principal modes of heat transfer prevalent in T_e models and expanded upon each one (Figure 4). My goal was to create a simple model that circumvented many of the empirically derived constants and measured variables that are common among other heat balance algorithms. However, the components of my model are

still based on models and explanations of previously published T_e calculations used to examine the responses of ungulates, wild and domestic, to heat stress.

Since I did not work directly with deer on Fire Island, and therefore did not obtain measurements from the animals themselves, all thermal constants used to represent them were taken from averages found in the literature, which are referenced in Table 2 and Appendix A. All other elements of the model are based on the physics of an organism receiving and losing heat throughout a given day until thermal equilibrium is reached, and how that energy flux is influenced by a certain environment, particularly in the thermal boundary layer (Moen and Jacobsen 1975). Since modeling heat exchange is incredibly complex, I have made a number of simplifying assumptions that are detailed below. Two measured variables considered as inputs to this computation were ambient temperature and steady wind speed, both of which were recorded by the stations.

The model in Eq. 1 was derived from the basic balance equation for heat transfer, where the algebraic sum of all the heat flow mechanisms is zero:

$$P_{Sun} + P_{Rad} + P_{Cond} + P_{Conv} = 0, \tag{2}$$

where P_{Sun} is the radiant solar power absorbed by the organism (W), P_{Rad} is the heat flow rate radiated from the organism (W), P_{Cond} is the heat flow rate conducted from the organism through the fur barrier (W) and P_{Conv} is the heat flow rate carried from the organism via air currents (W; Appendix A).

The first variable in Eq. 2, P_{Sun}, is the radiant solar power, or the solar radiant energy absorption rate of deer, which was calculated using the following equation:

$$P_{Sun} = P_{max}\varepsilon_D A_D \sin(\theta_{Sun}) , \quad if \ \theta_{Sun} \leq 0 \ then \ P_{Sun} = 0, \tag{3}$$

where P_{max} is maximum solar power density (Wm^{-2}), ε_D is the emissivity (0.97; the ratio of energy radiated from the coat of the deer to that radiated from a perfect blackbody), A_D is the effective thermal radiation area of the deer (1.5 m^2) and θ_{Sun} is the solar elevation angle (deg; Appendix A).

P_{max} calculates the maximum solar power density incident on the earth's atmosphere without obstruction and varies depending on the day of the year (Rai 1980). I only accounted for clear-sky radiation (i.e., no attenuation by atmospheric moisture, cloud or canopy cover). I chose to exclude these obstructions in the model for the sake of simplicity. I did not record any measurements of those variables on Fire Island since processing such data from remote sensing equipment would add too much complexity. Additionally, aside from sections of pine and holly groves, the majority of my study area is not covered by an obstructive tree canopy. The maximum solar power density equation multiplied a solar constant (1366 Wm^{-2}) by the varying albedo levels specific to each station (Rai 1980, Campbell and Norman 1998; Table 1). The solar elevation angle included calculations of the hour angle and solar declination based on a site latitude of 40.7° (Kumar et al. 1997, Campbell and Norman 1998, Sarbu and Sebarchievici 2017). I obtained the value for emissivity from Belovsky (1981), and the thermal radiation area of deer was determined to be the surface area of a 45-kg female deer (Moen 1973). I assumed, for simplification, that solar radiation is normally incident on the surface of the deer (i.e., 90°).

The second variable in Eq. 2, P_{Rad}, is the rate at which heat is radiated from the deer, and was calculated as:

$$P_{Rad} = -\varepsilon_D \sigma A_D T_a^4, \tag{4}$$

where σ is the Stefan-Boltzmann constant ($5.67 \cdot 10^{-8}$ Wm^{-2}K^{-4}). I developed this portion of the

model by examining other radiation components of heat balance models, specifically those from

Bakken (1976, 1992), Bakken et al. (1985) and Smith et al. (1985), which were primarily

focused on the explanation of T_e and predictions of shade-seeking behavior, respectively. This

equation represents the rate that heat is radiated away from the outermost surface of an organism,

or the Stefan-Boltzmann Law, which can be found in numerous other studies and textbooks that

use or explain thermal radiative heat transfer (Porter and Gates 1969, Moen 1973, Davis and

Birkebak 1975, Bunnell et al. 1986, Parker and Gillingham 1990, Sharpe and Van Horne 1999,

Hetem et al. 2007, Maia et al. 2014, 2016).

The third variable in Eq. 2, P_{Cond}, is the rate at which heat is conducted away from deer

through its fur barrier and was calculated as:

$$P_{Cond} = -\frac{K_{fur} A_D (T_e - T_a)}{f_D}, \tag{5}$$

where K_{fur} is the thermal conductivity of the deer's fur (3.56 Wm^{-1}K^{-1}; Davis and Birkebak

1975) and f_D is the fur thickness of a deer's coat in early fall (0.017 m; Moen 1973). Conduction

to the substrate is often seen as negligible and so is usually not included in the calculation of T_e.

For deer in particular, in addition to the small surface area in contact with the ground through the

hooves, the effect of conduction to the ground should be minimal because deer are not much

warmer than the surrounding environment at that particular contact point due to the

thermoregulatory process of countercurrent heat exchange. This strategy allows heat to be

exchanged between warm arterial blood passing from the body core and cold venous blood flowing up from the extremities (Marchand 2014). Instead, I incorporated conduction as a function of the heat carried through a deer's fur barrier, which is proportionately more relevant at very low wind speeds. Because fur is so difficult to model, I took an approach similar to Smith et al. (1985) and Kwak et al. (2016), where I assumed that a deer's fur was composed of a single material that was shallow and thermally passive (no heat generation or storage) and calculated the heat loss rate by dividing the conductivity of the deer's fur by the thickness of the fur. Additionally, as outlined in Smith et al. (1985), measurements of ground temperature are often required to determine the temperature of fur at other parts of the body besides an animal's horizontal back; however, there are few meteorological resources that provide those measurements, and modeling ground temperature requires extensive data on soil properties, which was beyond the scope of my project and is why I chose to treat the fur as a single thermal surface.

The final variable in Eq. 2, P_{Conv}, is the rate at which heat is carried away from deer by air currents via forced convection and was calculated as:

$$P_{Conv} = -\frac{K_{air} A_D (T_e - T_a)}{\delta_{BL}},\qquad(6)$$

where K_{air} is the thermal conductivity of air (0.025 Wm^{-1}K^{-1}) and δ_{BL} is the thermal boundary layer. I represented the flow of wind across and through the deer's fur as the distance across a thermal boundary layer from the deer to free stream ambient temperature using the Reynolds number. Calculation of the Reynolds number is a function of steady wind speed, fur thickness, dynamic viscosity, and density of air (Southwick and Gates 1975; Appendix A). Values for the

thermal conductivity, density and dynamic viscosity of air were retrieved from Touloukian et al. (1975). I aimed to represent a deer, which is made up of a variety of complex shapes, as a singularly simple surface, similar to explanations in Bakken and Gates (1975). For this reason, I treated the air flowing through its fur as a fluid flowing along a wall. When the fluid moves along the wall, the velocity of the flow asymptotically approaches the free stream velocity as distance from the wall increases (Janour 1951). The boundary layer is the middle layer (the deer's fur) between the upper layer (free stream air flow) and the lower layer (the deer's skin); this is illustrated in Figure 5. As the thickness of a deer's fur changes significantly over the seasons, the heat lost as a result of convection also changes. Although I only incorporated fur thickness in early fall, the model is meant to be easily modified and can be adjusted to account for varying fur thicknesses throughout the year, such as winter fur which can be 0.024 m thick (Moen 1973). For the purposes of the current model, convection was assumed to be forced across a laminar surface, or as convective transport to or from an animal's body. I did not account for free convection because the model was ultimately aimed at understanding shade-seeking behavior of deer, and deer are likely not searching for shade at night when free convection becomes a prevalent method of heat transfer. I also assumed that the deer was standing at all times and its posture was static.

I substituted Eq. 3, Eq. 4, Eq. 5 and Eq. 6 into Eq. 2 and solved for T_e to obtain Eq. 1. I then calculated T_e for nine stations on Fire Island using hourly aggregated data of ambient temperature and steady wind speed from January 2016 to January 2017. I developed an algorithm from these calculations which was implemented as an R script (version 3.6.3) of the applicable parametric equations, and I then exported the resulting T_e values into Excel

spreadsheets. Predicted T_e was plotted against measured Vernon globe temperature for stations with sufficient observations in order to validate the 127-mm globe (Appendix B).

RESULTS

Due to various sensor malfunctions, there was not a continuous record for any station throughout the duration of deployment. Although the most continuous record of data was from January 13, 2016 to January 31, 2017, not all of the stations had sufficient data throughout each month to compare Vernon globe temperature and modeled T_e over that time period. The availability of hourly data from each station in the sensor network over the 385 days is summarized in Table 3. Due to these gaps, three stations with adequate data were used to display the relationship between modeled T_e and measured Vernon globe temperature – Holly Grove, House and Pine Grove in April and July. April and July were chosen because they are two periods where deer are susceptible to thermal stress on Fire Island; deer experience cold stress in early April, and heat stress in late April and July. Holly Grove and Pine Grove were located in OPWA and House was located in Watch Hill. Mean wind speed was 0.64 ms^{-1} and 0.15 ms^{-1} in April and July, respectively. Mean ambient temperature was 8.93 °C and 23.03 °C in April and July, respectively. Measured Vernon globe temperatures ranged from -3.73 to 29.02 °C in April (Table 4) and 15.39 to 41.45 °C in July (Table 5), with means of 9.75 °C and 24.05 °C, respectively. Modeled T_e ranged from -4.07 °C to 21.32 °C in April (Table 4) and 14.04 to 34.94°C in July (Table 5), with means of 8.59 °C and 22.25 °C, respectively.

Vernon globe temperature and T_e followed the same cyclical pattern over the diel during both months, with peaks during the day and troughs at night (Figures 6A – 11A). Additionally, the difference in amplitude between the two variables was relatively small. The mean and maximum differences were also similar between the two months. The mean difference between

measured Vernon globe temperature and modeled T_e in April was 1.84, 1.61 and 1.64 °C for Holly Grove, House and Pine Grove, respectively, and 1.94, 1.78, and 2.31 °C in July, respectively. Measured Vernon globe temperature was predominately higher than modeled T_e at Holly Grove and Pine Grove in April and July, notably during the day, while the difference was less pronounced at House. In some instances during the day at House, modeled T_e was slightly higher than Vernon globe temperature in April and July. The maximum difference in April was 10.49 °C at Holly Grove (Figure 6B), 6.17 °C at House (Figure 8B) and 12.72 °C at Pine Grove (Figure 10B). The maximum difference between the two variables in July was 9.83 °C for Holly Grove (Figure 7B), 7.39 °C at House (Figure 9B) and 11 °C at Pine Grove (Figure 11B).

DISCUSSION

The 127-mm Vernon globe thermometer performed adequately as a T_e proxy for white-tailed deer on Fire Island. When measured Vernon globe temperature was plotted against modeled T_e for Holly Grove, House and Pine Grove, the maximum difference did not exceed 13 °C and the mean difference did not exceed 3 °C. In terms of measured quantities, there were no significant disparities between wind speed, ambient temperature or Vernon globe temperature between Holly Grove, House and Pine Grove in either April or July. Mean T_e values were also very similar among the three stations in their respective months. While past studies measured T_e directly with thermal mounts, smaller and less expensive surrogates such as Vernon globes have been employed, and a suite of mathematical heat transfer equations and microclimate models united via computer software have updated the way the metric is calculated and visualized (Bakken et al. 1985, Dzialowski 2005, Elmore et al. 2017).

The thermal environment experienced by animals is the result of complex exchanges between solar and thermal radiation, wind speed, cloud, vegetative and topographical cover, the

animal's orientation, posture, body size and shape, as well as pelage color and thickness, among other factors (Bakken et al. 1985, Walsberg 1992, Mysterud and Østbye 1999). The rates of heat transfer within these environments are further dependent on the behavioral and physiological mechanisms employed by the animal, which, in hostile environments, often result in trading-off critical activities such as forage-seeking for thermoregulation (McCain and King 2014, Maia et al. 2016). Operative temperature represents these elements and exchanges among the thermal environment experienced by an animal as a single number (Bakken 1992, Dzialowski 2005).

One of the prominent models of T_e was published by Parker and Gillingham (1990) for mule deer (hereafter referred to as the PG model). I derived many of the elements for my own model from this study; however, my version is more simplified. One such simplification is that while my model utilized steady wind speed and ambient temperature as the primary drivers in the calculation of T_e, it did not account for scattered and diffuse solar radiation. I did not have the instrumentation nor means to obtain these values, so I took a more direct approach by combining both long and shortwave radiation into a single variable to represent the maximum solar radiant energy incident on the atmosphere. Another alteration involved the calculation for resistance to forced convective heat transfer found in PG's model. This component involved dividing the characteristic dimension of the animal by the wind speed and then taking the square root of that quantity. When wind speed is zero, T_e becomes undefined. An equation that breaks down at its boundary condition presents challenges when the inputs for that variable are not assumed to be constant. The model I developed is able to handle wind speeds of 0 ms^{-1}, which often occurs in the large data set used for the T_e calculations. While there are ways to exclude this particular wind speed, I found that it was easier to allow the model to account for wind speeds of zero as well as the effect of high wind speeds, rather than use a wind speed correction

factor as in the PG model. An additional adjustment was in the calculation for direct beam radiation on a surface perpendicular to the beam. This component of the PG model included an equation where the incident beam radiation was divided by the sine of the solar angle, causing the value of T_e to skyrocket at shallow elevation angles. In order to avoid this issue, I mathematically constrained the radiant solar power to zero watts when the sun angle is less than or equal to zero degrees (Appendix A).

The PG model is likely more accurate since it incorporates and accounts for more layered elements of the surrounding thermal environment and heat exchange of its subject organism, particularly in the form of solar radiation and thermal resistance. However, a possible advantage of my simpler model is that making modifications is inherently easier. My model includes many features similar to those found in the PG model and other models of T_e, but because modeling the thermal environment is an exceptionally challenging task, I found that beginning with fundamental energy relationships and building upon it for my specific case study, as per the advice of Moen (1973) and O'Connor and Spotila (1992), was more effective than navigating through and adjusting the multitude of empirical constants, formulas and units of the PG model. Simplified models are often useful in isolating important mechanisms and the weight of their role in the system, the organism(s), and interaction between the two. They can also be used to justify why certain elements were included while others were excluded and can help the researcher home in on the primary question that is attempted to be answered.

Measured Vernon globe temperatures were frequently higher than modeled T_e, notably when the sun was above the horizon at Holly Grove and Pine Grove (Figures 6A, 7A, 10A, 11A), whereas the NPS unit over House mostly ameliorated this effect (Figures 8A, 9A). One possible explanation for these differences is the variation in structural and environmental

conditions between site locations due to their placement in the natural versus built environments, resulting in differing vegetation composition, albedo, wind speed, ambient temperature and solar radiation values. While Holly Grove and Pine Grove were placed in partial shade within maritime forests in the OPWA, two natural areas undisturbed by human development, House was placed in a developed area with minimal surrounding vegetation and complete overhead obstruction from solar radiation. It is also important to note that the albedo values I chose for each site were based on values for similar surfaces, such as dry, white sand and dry, dark soil (Campbell and Norman 1998). However, these surfaces change throughout the year as vegetation grows and dies and soil is not always wet or dry, so the values may have to be adjusted depending on the conditions for the particular month being modeled.

Exposure to high levels of solar radiation during the day may be one of the reasons for such high values of Vernon globe temperature seen at Holly Grove and Pine Grove, as the globes fully absorb incoming radiation. Smith et al. (1985) also found values from their heat balance model often underpredicted at points with high levels of solar radiation when comparing predicted and measured wooltip temperatures on different positions of a sheep's torso. Similarly, in a comparison between T_e values registered from a black metal sphere and a taxidermic mount of a red-winged blackbird (*Agelaius phoeniceus*), Bakken et al. (1985) determined that the increased solar heating of the sphere caused the sphere temperatures to be higher than those of the mount at high values of T_e, whereas there was greater agreement between the sphere and mount temperatures at lower values of T_e. While this issue is likely unavoidable due to the absorption properties of the sphere, obtaining measurements of radiation through the various forms of canopy cover for each individual station and adjusting the solar radiation equations to account for those varieties may provide a more accurate calculation for modeled T_e. Calibrating

the models by comparing measured Vernon globe temperatures and modeled T_e values to the temperature of a live deer at thermal equilibrium may also help determine the accuracy of both models and determine acceptable margins of errors (Dzialowski 2005).

Neither Vernon globe temperatures nor models of T_e can account for all of the components and processes that influence how an organism perceives its environment, thus the absence of some of these elements such as cloud cover, atmospheric particles, elevation and canopy type in my model may have also caused the variation seen between measured Vernon globe temperature and modeled T_e. Furthermore, ambient temperature and wind speed were measured as a function of elevation and location, contributing to uncertainty in the model's application.

While globes present a robust, compact way to estimate T_e in the field, they fully absorb incident solar radiation, resulting in greater variation when compared to a measurement such as ambient temperature that only partially accounts for radiation, and do not account for the pelage properties (i.e., fur) or the complex geometry of an individual animal, possibly leading to less accurate measurements when compared to results acquired from taxidermic mounts of the animal (Dzialowski 2005). In some cases, painting a physical model with the aim of matching an animal's absorptivity can lead to inaccurate estimates of T_e in full and partial sun conditions, and there has been evidence that T_e values obtained from cylinder models that differed in absorptivity from the animal varied up to 12.5 °C under high solar radiation conditions (Bakken and Gates 1975, Dzialowski 2005). Nonetheless, globes and other small models are less expensive to construct, can be easily moved and attached to numerous micrometeorological stations and have been successfully used to estimate T_e (Hetem et al. 2007, Wiemers et al. 2014, Elmore et al. 2017), and may even provide better estimates when compared to a taxidermic

mount than would a copper model resembling the animal, as was the case in Bakken et al. (1985).

Mathematical versions of modeled T_e integrate several fundamental forms of heat exchange, physical organism traits, and measurements of spatio-temporal microclimates that can provide valuable insight into the processes that are important to an organism's interaction with the thermal environment. These models can also be utilized to predict T_e under theoretical future scenarios, but these values must be computed (Huey 1991) and rely on numerous assumptions and simplifications. Both types of models have flaws, yet they are useful in making inferences about the role of temperature on an organism.

While improvements continue to be made to these types of models, it is important to note that many of the parameters used in models of T_e are determined through laboratory-based experiments or estimates based on what is known about the animal and its environment. I have chosen to use Vernon globe temperature as a surrogate for T_e; however, this is not universally accepted. Despite this, I believe the utility of the model is apparent since it incorporates the fundamental mechanisms of heat transfer present between an animal and its environment. Additionally, predicted T_e values successfully followed the peaks and troughs of observed Vernon globe temperature over the diel and the simple nature of the model allows it to be modified to address more specific conditions at the site locations if necessary.

In addition to the calculated components, there were challenges with the measured variables. All of the micro-meteorological stations were on Fire Island for over three years. Although trips were made to replace batteries and repair hardware, the stations were still subjected to the harsh environment across the seashore including high winds, salt spray and freezing and extremely high temperatures. Wildlife interference with the equipment was also a

possibility. Due to exposure to the elements, there were several hardware failures that resulted in a discontinuous record of data for the different measurements from the date of deployment to the date that the stations were permanently removed. House was the only station that had a continuous record from the starting point to the end date (January 13, 2016 to January 31, 2017). Suggestions for addressing this problem and future work are discussed in the Epilogue.

Understanding the movement patterns of an animal that is well-equipped to not only survive but thrive in heavily populated human communities will be necessary to develop strategies that effectively maintain healthy ecosystems and allow people and deer to coexist on Fire Island. According to the White-tailed Deer Management Plan this involves reducing direct human-deer interactions by achieving a target of 20 to 25 deer per square mile throughout federally designated land, which will protect and aide in the restoration of Sunken Forest and other maritime forests across the seashore that support deer, birds, insects, amphibians, reptiles, and other small mammals (NPS 2019b). Despite the fact that many elements of the landscape (e.g., ambient temperature) cannot be directly controlled, identifying thermal thresholds can help predict where organisms may seek refuge when experiencing heat stress (Roberts et al. 2016, Thaker et al. 2019). Linking the influence of temperature to a species with knowledge of their biology is more likely to provide benefits to management rather than simply using reports of average conditions to develop predictions on space-use and patterns; this is especially true because of the multitude of factors that drive abundance, such as life history, competition and habitat quality (Dawe and Boutin 2016, Elmore et al. 2017).

While many species will be threatened with extinction in the wake of range shifts driven by climate change, deer on Fire Island have the unique opportunity to further exploit nearby human-dominated landscapes in order to alleviate thermal stress. In addition to relief from

convective and radiative heat losses or gains, the built environments on Fire Island also provide escape from biting insects and parasites, and greater access to substantial and nutritious forage. However, the overabundance of deer across the seashore has ultimately resulted in numerous short and long-term ecological impacts and elevated concern about the spread of tick-borne illnesses, notably Lyme disease, as warmer temperatures are likely to create more favorable environments for the black-legged tick (*Ixodes scapularis*) and other parasites that spend the majority of their life cycle away from their host (Brownstein et al. 2005, NPS 2019b). Furthermore, decades of unremitted browsing on low-lying saplings and seedlings have prevented the development of fully functional forest ecosystems that would normally not provide enough food to support large populations, and threatens rare, old-growth vegetation communities as well as the wildlife they sustain (Forrester et al. 2006, Rawinski 2008). This lack of forest regeneration leaves openings for exotic plant species, and the availability of high-quality forage in the form of decorative landscaping plants combined with the complete absence of predators further exacerbates the problem (Department of Environmental Conservation 2018a, NPS 2019b).

There are few studies to date that examine the influence of temperature and the consequences of thermoregulation on a ubiquitous ungulate that successfully inhabits a locale containing both natural and densely populated residential communities with no predators and abundant resources. Dawe and Boutin (2016) modeled the impact of climate change and human land use patterns on deer distribution; however, this examination took place in Alberta, Canada which does not compare well to Fire Island based on the significant difference in available area between the two locations. Additionally, Alberta and other northern Canadian territories do not have the level of anthropogenic development or population that Fire Island does. Even if there

was significant industrial expansion in Canada, the difference in the degree to which such development would influence deer distribution compared to Fire Island would be too great. Both behavioral and physiological adaptations are likely to play a role in buffering mammals against climate change. However, white-tailed deer are in a unique position where they may actually benefit from these effects given their ability to navigate and thrive in human-dominated landscapes. In order to develop effective predictive models to understand the response and capacity of movement of deer, information about changes to habitat structures and microclimates, trophic interactions and ecological energetics must be incorporated (Fuller et al. 2016).

As temperatures increase, identifying key thermal refuges for deer in predator-absent, human-dominated communities will become increasingly important, particularly given evidence that deer will move out of natural areas into residential communities (Walker 2006). My model was built to obtain calculations of the thermal environment experienced by deer based on their physiological and morphological characteristics, and the exchanges with the abiotic elements of the environment, namely solar radiation, wind speed and ambient temperature. It is possible that these results could be used to highlight areas of optimal T_e. Operative temperature is an index that can be visually represented on thermal maps, which will not only help distinguish suitable from unsuitable habitats, but also highlight changes in the distribution of those habitats over time (Dzialowski 2005). Isolating areas that are likely to experience the impacts of deer most heavily will be useful for managers that need to mediate conflicts and provision resources between people and wildlife, conserve important old-growth forest and other plant communities that help sustain wildlife, and preserve natural and economic resources important to the general public throughout the island. Understanding the space use patterns of deer based on their interaction

with the thermal environment and behavioral and physiological adaptations in a changing

landscape, in both a climate and a land use-sense, is crucial for current and future management.

These findings may be useful in future plans for managing deer distribution and density on Fire

Island.

Table 1. Location, elevation, albedo and total number of useable observations of micrometeorological stations that measured ambient temperature, Vernon globe temperature and steady and gust wind speeds on Fire Island from January 12, 2016 to July 14, 2018.

Name	Latitude (dec. deg.)	Longitude (dec. deg.)	Elevation (m)	Albedo*	Total number of useable observations*
Base Station	40.691	-72.989	0.8	-	55,440
High Dune	40.704	-72.950	9.3	0.35	55,440
Holly Grove	40.693	-72.983	1.6	0.15	95,444
House	40.690	-72.991	0.7	0.13	116,297
Low Dune	40.689	-72.990	7.7	0.35	55,440
Marsh	40.693	-72.985	0.4	0.10	55,440
Overwash	40.706	-72.947	2.2	0.30	55,440
Phrag	40.691	-72.989	0.5	0.16	55,440
Pine Grove	40.704	-72.954	1.1	0.15	131,373
Swale	40.688	-72.994	1.4	0.26	131,478

* Albedo values were determined for each station based on values for similar surfaces found in Campbell and Norman (1998).

* Total number of useable observations was acquired from the data collected at 10-minute intervals before it was aggregated by the hour and included NA values within the 385 days used for analysis.

Table 2. Inputs to a model of operative temperature (T$_e$) for white-tailed deer.

Constants, Variables and Equations	Source	Reference
Ambient temperature (T_a; K)	Measured by micro-meteorological stations	
Radiant solar power (P_{Sun}; W)	$P_{max}\varepsilon_D A_D \sin(\theta_{Sun})$ if $\theta_{Sun} \leq 0$ $then$ $P_{Sun} = 0$	Rai 1980, Campbell and Norman 1998
Maximum solar power density (P_{max}; Wm^{-2})	$G_S(1-\varepsilon_S)\left[1 + 0.033\, cos\left(\dfrac{2\pi(n-4)}{365}\right)\right]$	Rai 1980
Solar constant (G_S)	$1.366 \cdot 10^3$ Wm^{-2}	Rai 1980
Albedo (ε_S)	Variable based on micro-meteorological station	Campbell and Norman 1998
Day of the year (n)	1 - 365	
Emissivity of surface (ε_D)	0.97	Belovsky 1981
Effective thermal radiation area (A_D)	1.5 m^2	Moen 1973
Solar elevation angle (θ_{Sun}; deg)	$\sin^{-1}\left[\sin(\theta_{Lat})\,\sin(\theta_{Dec}) + \cos(\theta_{Lat})\,\cos(\theta_{Dec})\,\cos(\theta_{Hour})\right]$	Campbell and Norman 1998
Data site latitude (θ_{Lat})	40.7°	
Data site declination (θ_{Dec}; deg)	$23.45 \sin\left[\left(\dfrac{360}{365}\right)(n + 284)\right]$	Kumar et al. 1997, Sarbu and Sebarchievici 2017
Hour angle (θ_{Hour}; deg)	$15(t_{Hour} - 12)$	Campbell and Norman 1998
Local time of day (t_{Hour}; hr)	$0 \leq t_{Hour} < 24$	
Rate heat is radiated from deer (P_{Rad}; W)	$\varepsilon_D \sigma A_D T_a^4$	Bakken 1976, 1992, Smith et al. 1985
Stefan-Boltzmann constant (σ)	$5.67 \cdot 10^{-8}$ Wm^{-2} K^{-4}	Bakken 1992
Conductive heat loss rate (P_{Cond}; W)	$\dfrac{K_{fur}A_D(T_e - T_a)}{f_D}$	Moen 1973, Bakken and Gates 1975, Smith et al. 1985
Thermal conductivity of fur (K_{fur})	3.56 Wm^{-1}K^{-1}	Davis and Birkebak 1975
Fur thickness of deer (f_D)	0.017 m in early fall	Moen 1973
Convective heat loss rate (P_{Conv}; W)	$\dfrac{K_{air}A_D(T_e - T_a)}{\delta_{BL}}$	Moen 1973, Bakken and Gates 1975, Smith et al. 1985, Bakken 1992
Thermal conductivity of air (K_{air})	0.025 Wm^{-1}K^{-1}	Touloukian et al. 1975
Thermal boundary layer (δ_{BL}; m)	$5.2\dfrac{f_D}{\sqrt{Rn}}$	Janour 1951
Reynolds number (Rn)	$\dfrac{\rho_{air}V_W f_D}{\mu_{air}}$ if $V_W \leq 0$ $then$ $Rn = 0.001$	Southwick and Gates 1975
Density of air (ρ_{air})	1.22 kg m^{-3}	Touloukian et al. 1975
Wind velocity (V_W; ms^{-1})	Measured by micro-meteorological stations	
Dynamic viscosity of air (μ_{air})	$1.80 \cdot 10^{-5}$ kg m^{-1}s^{-1}	Touloukian et al. 1975

Table 3. Summary of hourly data available from each station in the sensor network from January

13, 2016 to January 31, 2017.

Names	Comments
High Dune	NAs from hour 0 of 1/13/16 through hour 15 of 4/26/16 Data from hour 16 of 4/26/16 through hour 7 of 1/11/17 NAs from hour 8 of 1/11/17 through hour 23 of 1/31/17 for wind and gust speed when anemometer fails; Vernon globe and ambient temperature measured through hour 23 of 1/31/17
Holly Grove	NAs from hour 0 of 1/13/16 through hour 14 of 1/13/16 Continuous record from hour 15 of 1/13/16 through hour 23 of 1/31/17
House	Continuous record of data from hour 0 of 1/13/16 through hour 23 of 1/31/17
Low Dune	NAs from hour 0 of 1/13/16 through hour 13 of 1/14/16 Data from hour 14 of 1/14/16 through hour 13 of 5/15/16 NAs from hour 14 of 5/15/16 through hour 12 of 9/11/16 Data from hour 13 of 9/11/16 through hour 20 of 1/24/17 NAs from hour 21 of 1/24/17 through hour 23 of 1/31/17
Marsh	NAs from hour 0 of 1/13/16 through hour 11 of 4/27/16 Data from hour 12 of 4/27/16 through hour 16 of 5/2/16 NAs from hour 17 of 5/2/16 through hour 23 of 1/31/17 for wind and gust speed when anemometer fails; Vernon globe and ambient temperature sensors fail at hour 16 of 5/4/16 through hour 23 of 1/31/17
Overwash	NAs from hour 0 of 1/13/16 through hour 14 of 4/26/16 Data from hour 15 of 4/26/16 through hour 9 of 6/2/16 NAs from hour 10 of 6/2/16 through hour 15 of 9/11/16 Data from hour 16 of 9/11/16 through hour 11 of 10/17/16 NAs from hour 12 of 10/17/16 through hour 23 of 1/31/17
Phrag	NAs from hour 0 of 1/13/16 through hour 10 of 4/27/16 Data from hour 11 of 4/27/16 through hour 15 of 4/27/16 NAs from hour 16 of 4/27/16 through hour 13 of 9/11/16 Data from hour 14 of 9/11/16 through hour 19 of 9/11/16 NAs from hour 20 of 9/11/16 through hour 23 of 1/31/17
Pine Grove	NAs from hour 0 of 1/13/16 through hour 8 of 1/15/16 Data from hour 9 of 1/15/16 through hour 9 of 3/24/16 NAs from hour 10 of 3/24/16 through hour 13 of 3/24/16 Data from hour 14 of 3/24/16 through hour 23 of 1/31/17
Swale	NAs from hour 0 of 1/13/16 through hour 9 of 4/27/16 Data from hour 10 of 4/27/16 through hour 23 of 1/31/17

Table 4. Mean, minimum and maximum values of wind speed (ms^{-1}), ambient temperature (°C) and Vernon globe temperature (°C) collected from micrometeorological stations and modeled T_e (°C) in April 2016 for three stations.

Variable	Station	Mean	Minimum	Maximum
	Holly Grove	0.45	0	2.73
Wind speed	House	0.54	0	3.30
	Pine Grove	0.93	0	5.14
	Holly Grove	8.85	-2.28	19.17
Ambient temperature	House	8.64	-2.36	18.85
	Pine Grove	9.29	-2.67	19.62
	Holly Grove	10.12	-2.45	29.02
Vernon globe temperature	House	9.14	-1.85	20.24
	Pine Grove	9.97	-3.73	28.74
	Holly Grove	8.50	-3.69	21.15
Operative temperature	House	8.34	-3.70	20.65
	Pine Grove	8.93	-4.07	21.32

Table 5. Mean, minimum and maximum values of wind speed (ms^{-1}), ambient temperature (°C) and Vernon globe temperature (°C) collected from micrometeorological stations and modeled T_e (°C) in July 2016 for three stations.

| Variable	Station	Mean	Minimum	Maximum
Wind speed	Holly Grove	0.06	0	0.76
	House	0.06	0	1.20
	Pine Grove	0.34	0	1.77
Ambient temperature	Holly Grove	23.15	16.89	31.94
	House	22.83	16.57	30.04
	Pine Grove	23.11	15.87	32.34
Vernon globe temperature	Holly Grove	24.23	16.40	40.04
	House	23.32	16.80	30.75
	Pine Grove	24.60	15.39	41.45
Operative temperature	Holly Grove	22.36	15.03	34.32
	House	22.07	14.72	32.59
	Pine Grove	22.32	14.04	34.94
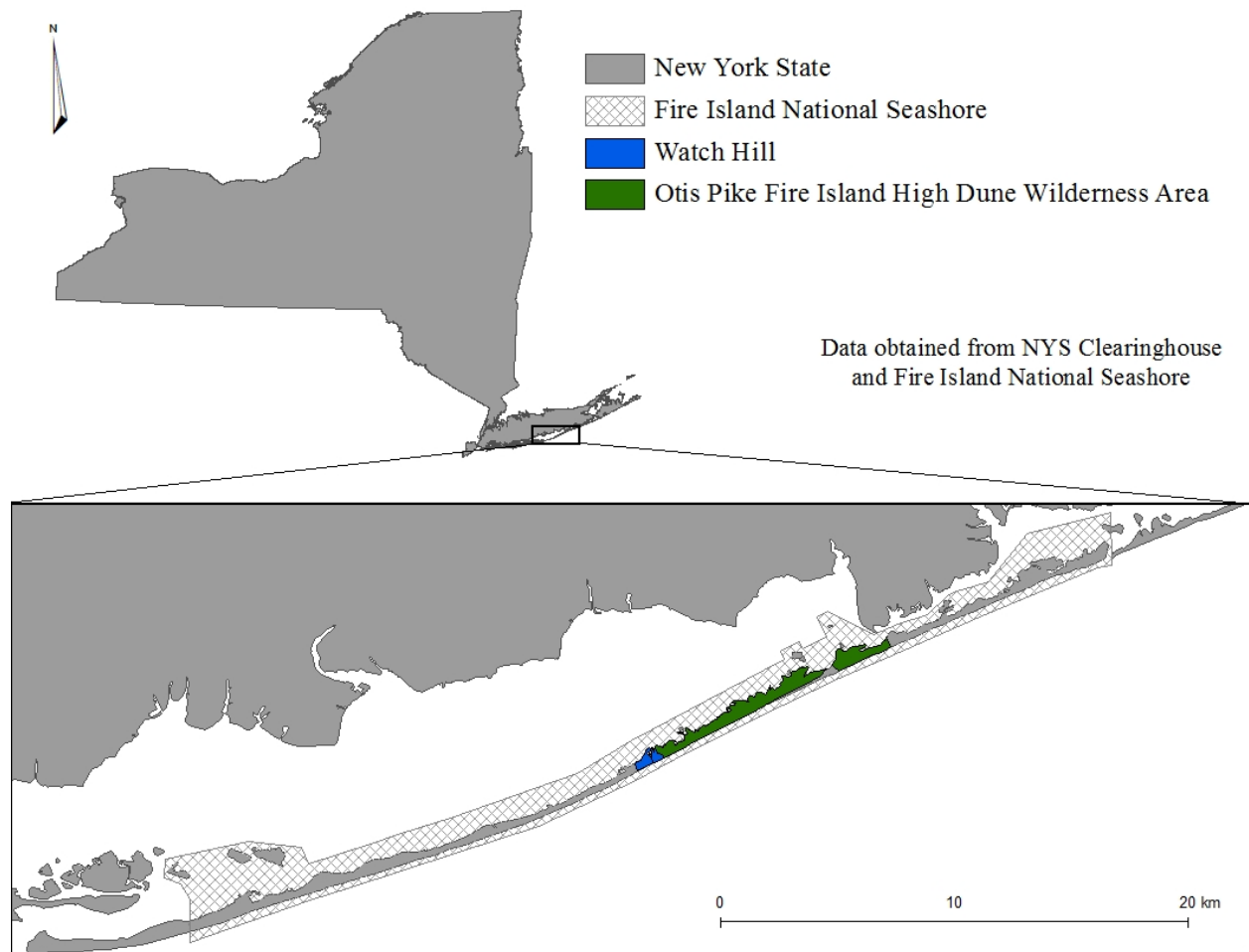
Figure 1. Location of Fire Island National Seashore, Watch Hill and the Otis Pike Fire Island
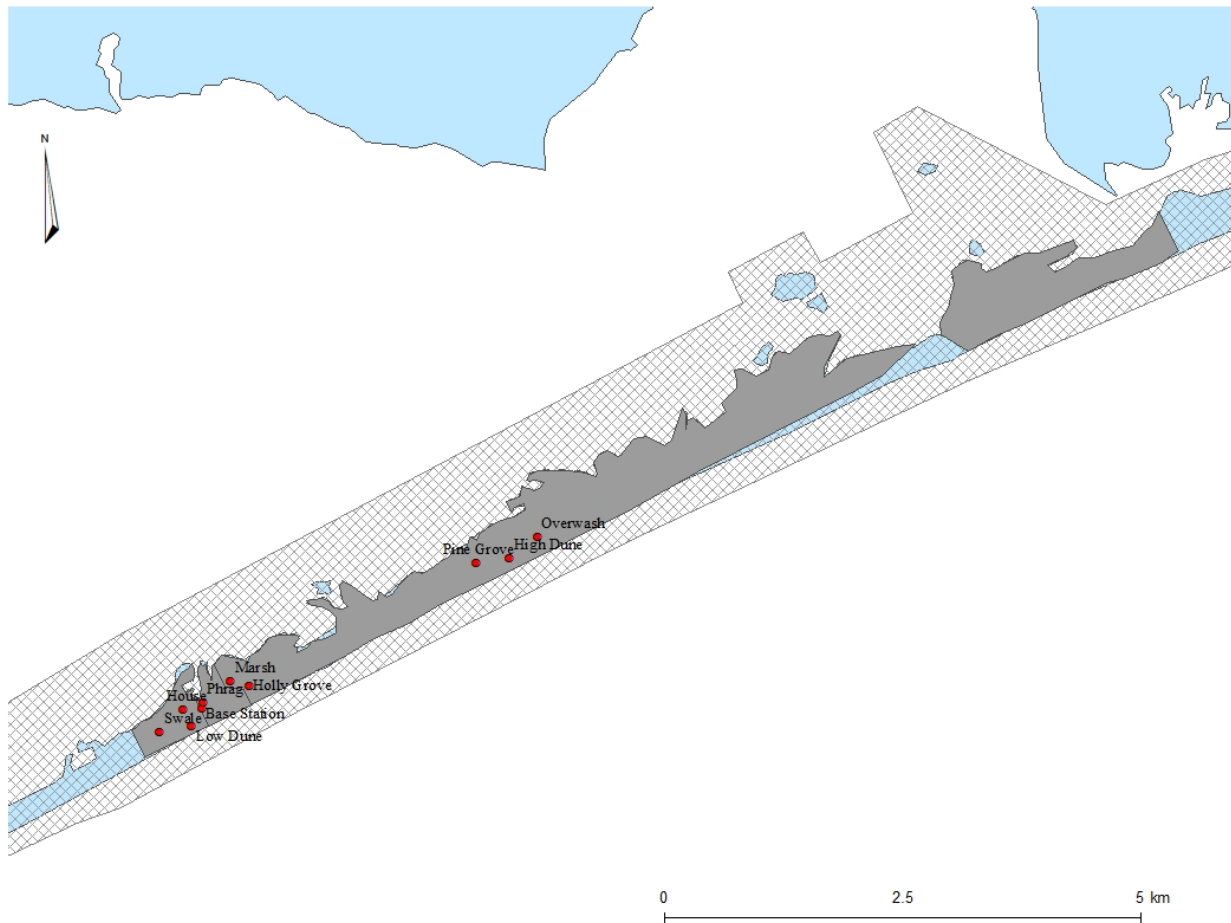
High Dune Wilderness Area, New York, USA.

Figure 2. Locations of the ten micrometeorological stations on Fire Island. The Otis Pike High Dune Wilderness Area breach at Old Inlet that occurred as a result of Hurricane Sandy on October 29, 2012 is displayed near the eastern end of the wilderness area. The breach connects the Atlantic Ocean to Great South Bay.

Figure 3. Vernon globe thermometers that were mounted on each station. Each copper sphere was painted matte black and contained an Onset 12-bit Smart Sensor thermistor.

**Maximum direct solar radiant power density incident on earth's atmosphere:
Solar constant (~ 1366 Wm^{-2})**

**Conductive heat loss rate:
heat conducted from deer through fur barrier**

**Radiation heat loss rate:
heat removed from deer by radiation**

**Convective heat loss rate:
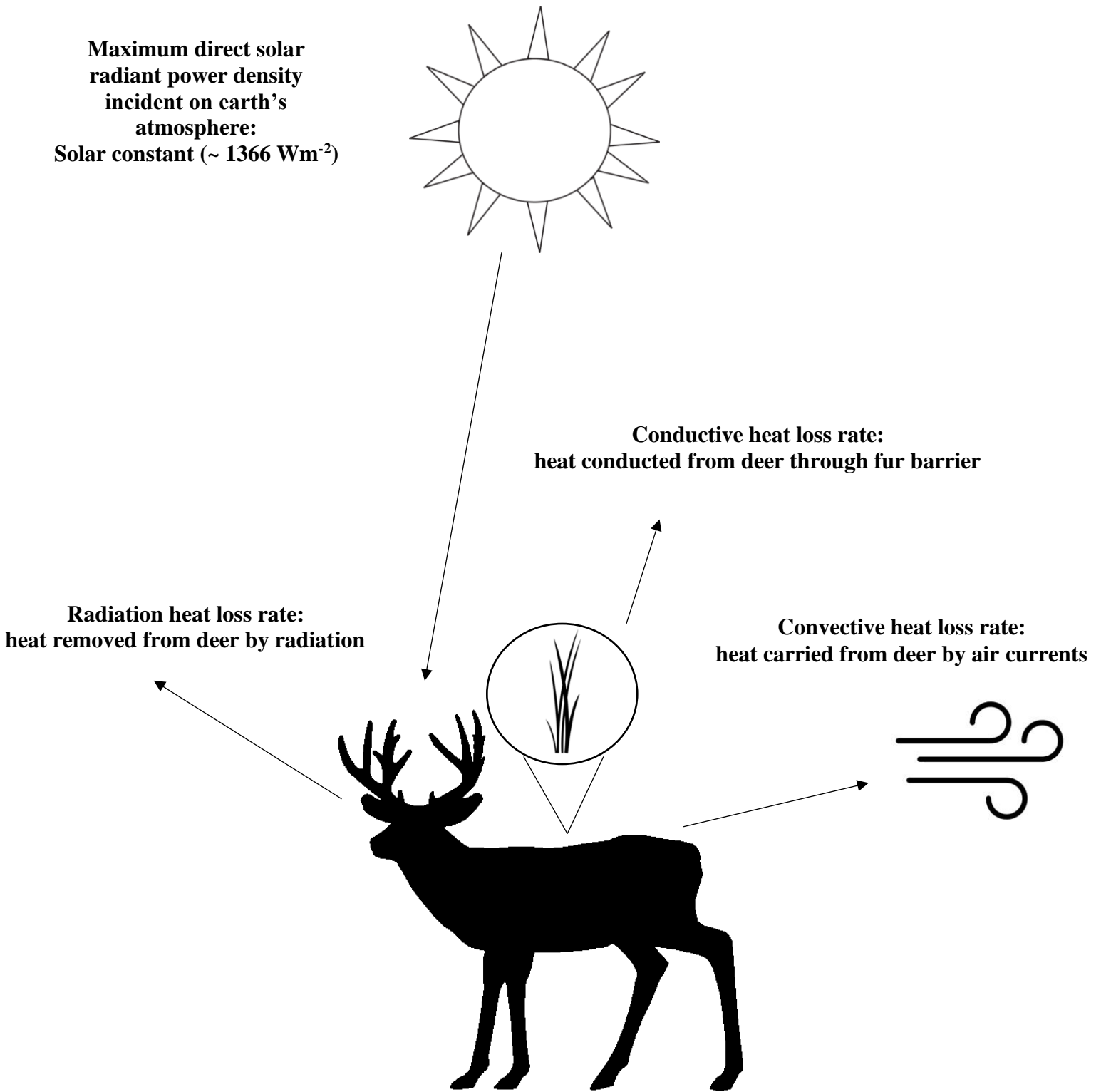heat carried from deer by air currents**

Figure 4. Four principal forms of heat transfer used in operative temperature (T$_e$) model.
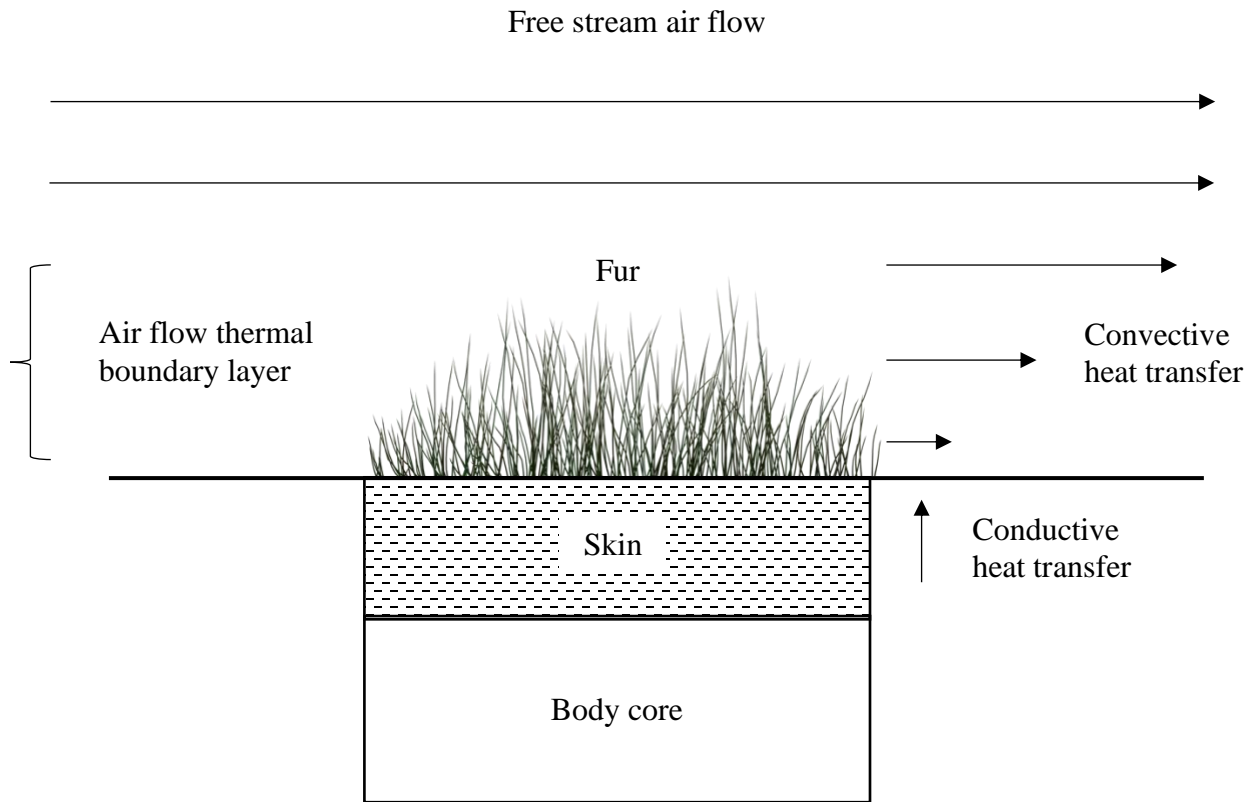
49

Figure 5. Representation of heat balance from body core to thermal boundary layer in T_e model. The varying arrow lengths displaying convective heat transfer indicate differences in air flow speed – zero at the skin surface, maximum above the fur. Conductive heat transfer is presented as the heat conducted from the surface of skin directly to the air through the fur barrier.
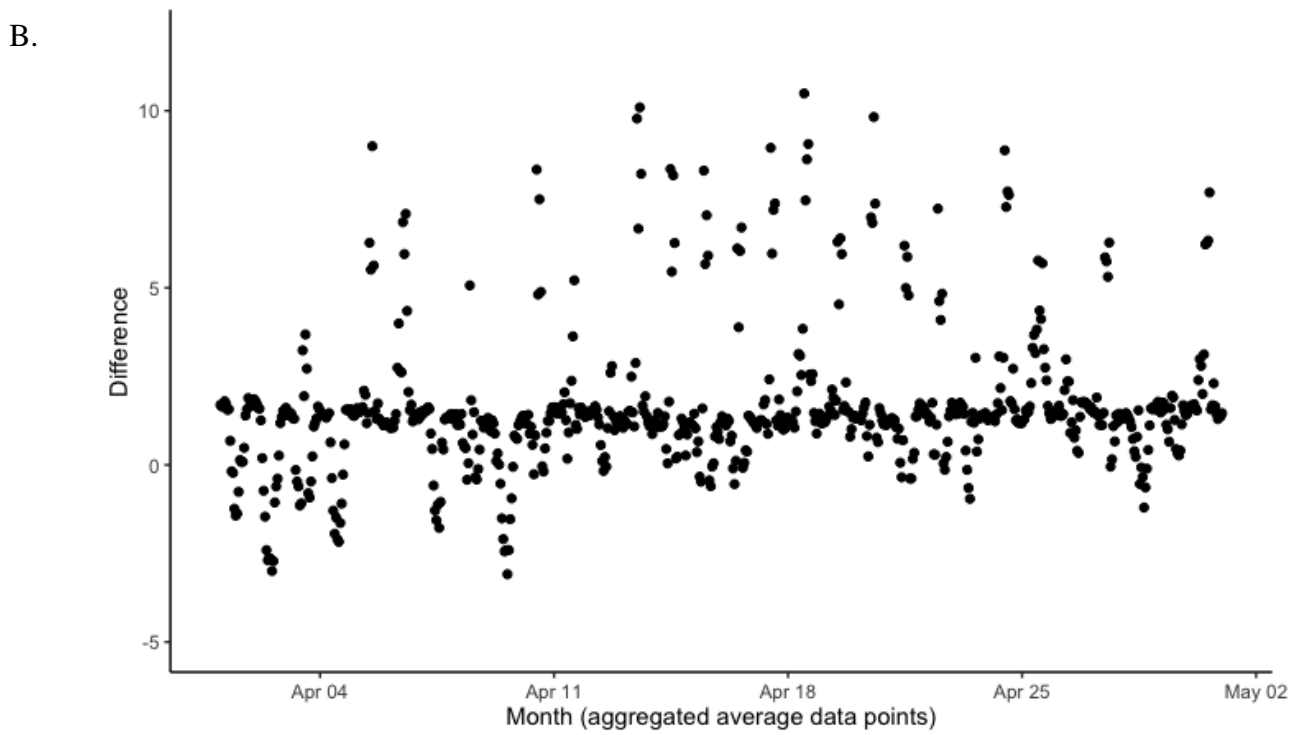
Figure 6. Relationship (A) and difference (B) between measured Vernon globe temperature (VGT) and modeled T_e over the month of April 2016 at the Holly Grove station in the OPWA, Fire Island, New York.

A.

B.

Figure 7. Relationship (A) and difference (B) between measured VGT and modeled T_e over the

month of July 2016 at the Holly Grove station in the OPWA, Fire Island, New York.

A.

B.
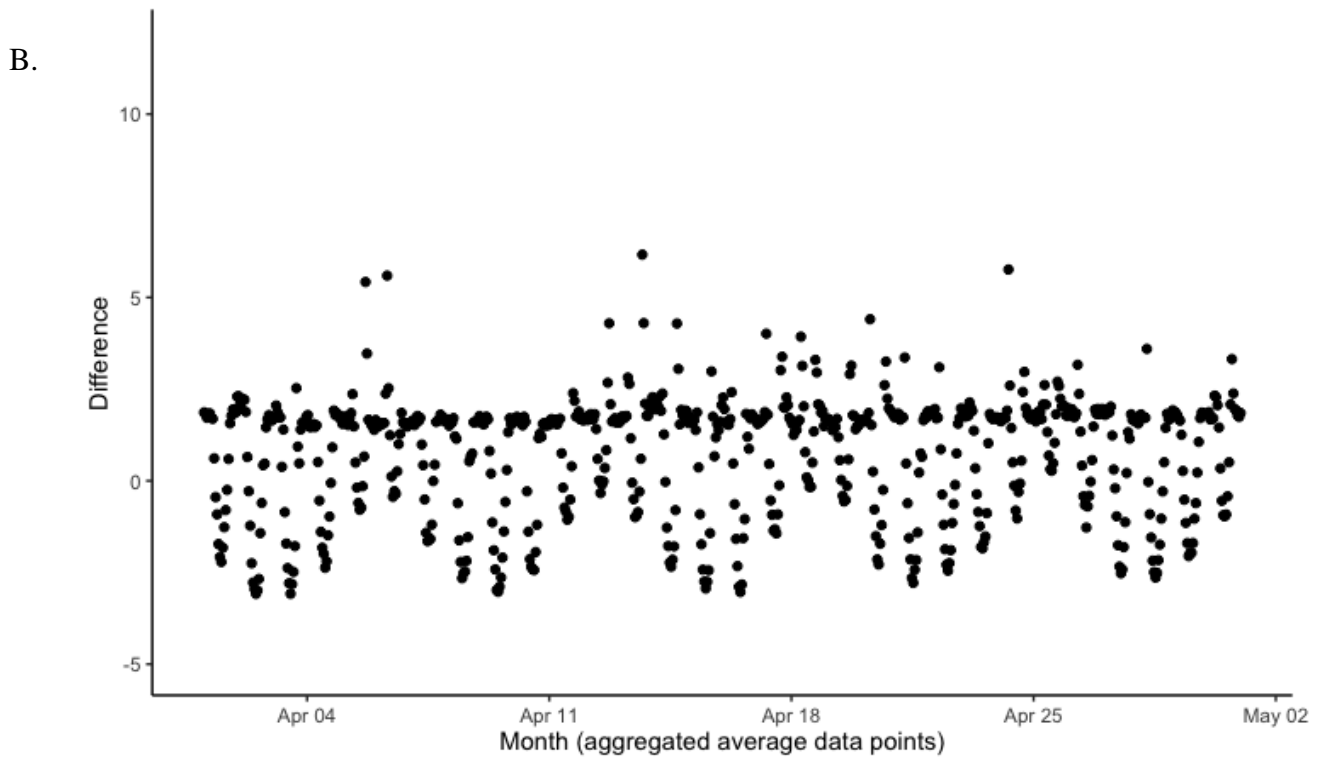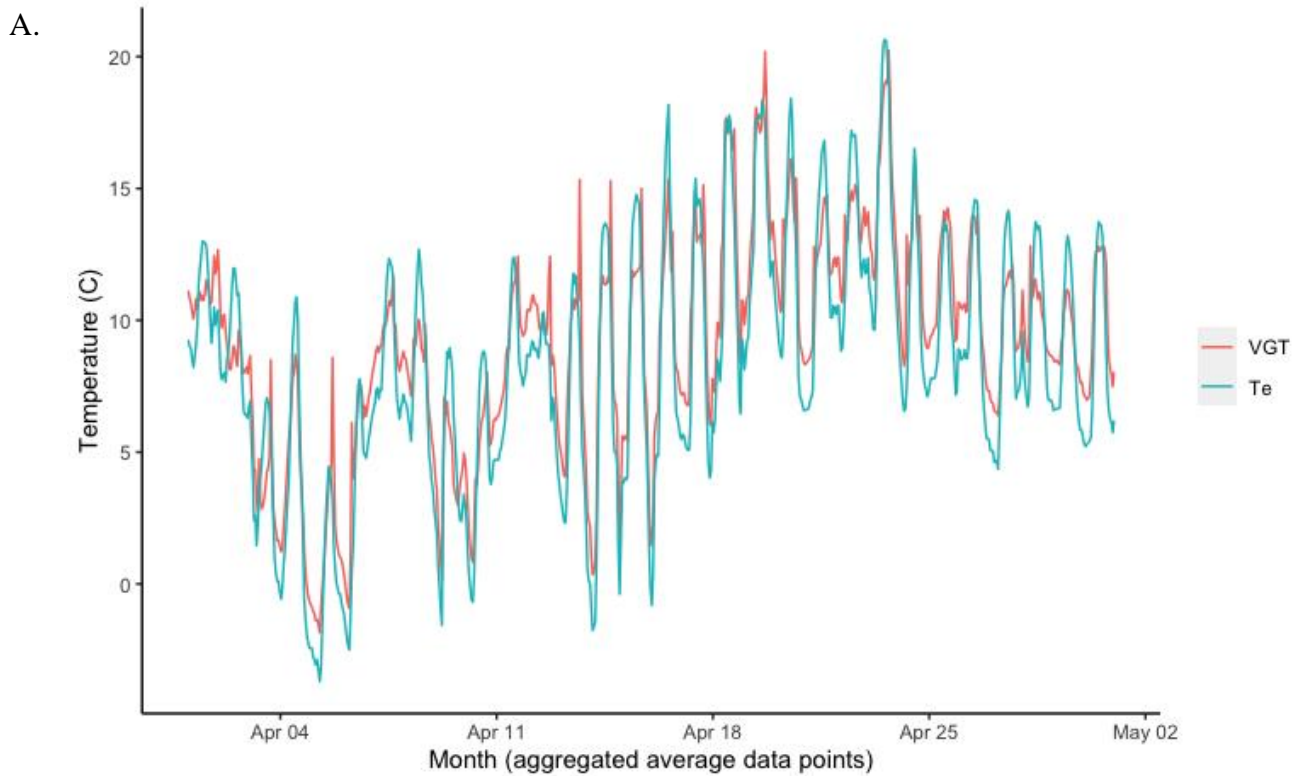
Figure 8. Relationship (A) and difference (B) between measured VGT and modeled T_e over the month of April 2016 at the House station in Watch Hill, Fire Island, New York.

Figure 9. Relationship (A) and difference (B) between measured VGT and modeled T_e over the month of July 2016 at the House station in Watch Hill, Fire Island, New York.

A.

B.
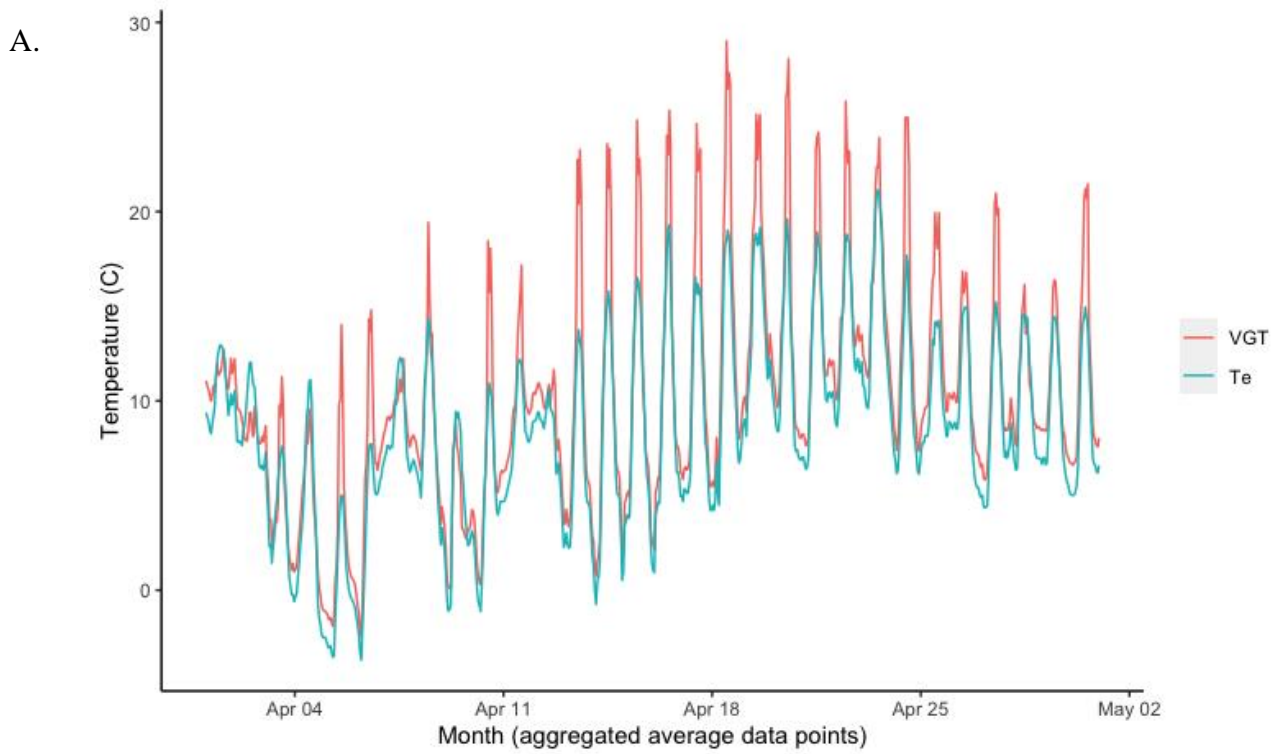
Figure 10. Relationship (A) and difference (B) between measured VGT and modeled T_e over the month of April 2016 at the Pine Grove station in the OPWA, Fire Island, New York.
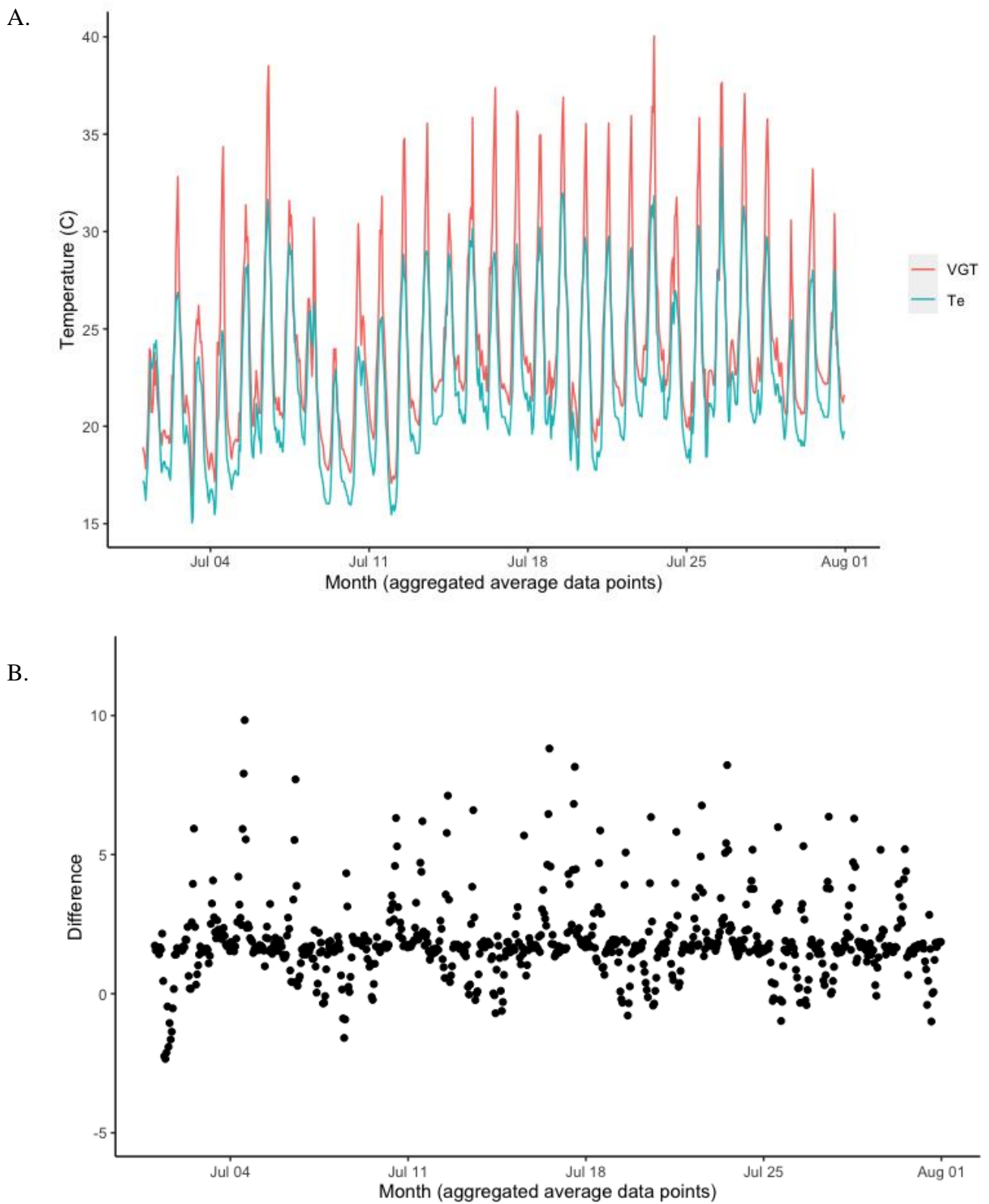
Figure 11. Relationship (A) and difference (B) between measured VGT and modeled T_e over the month of July 2016 at the Pine Grove station in the OPWA, Fire Island, New York.
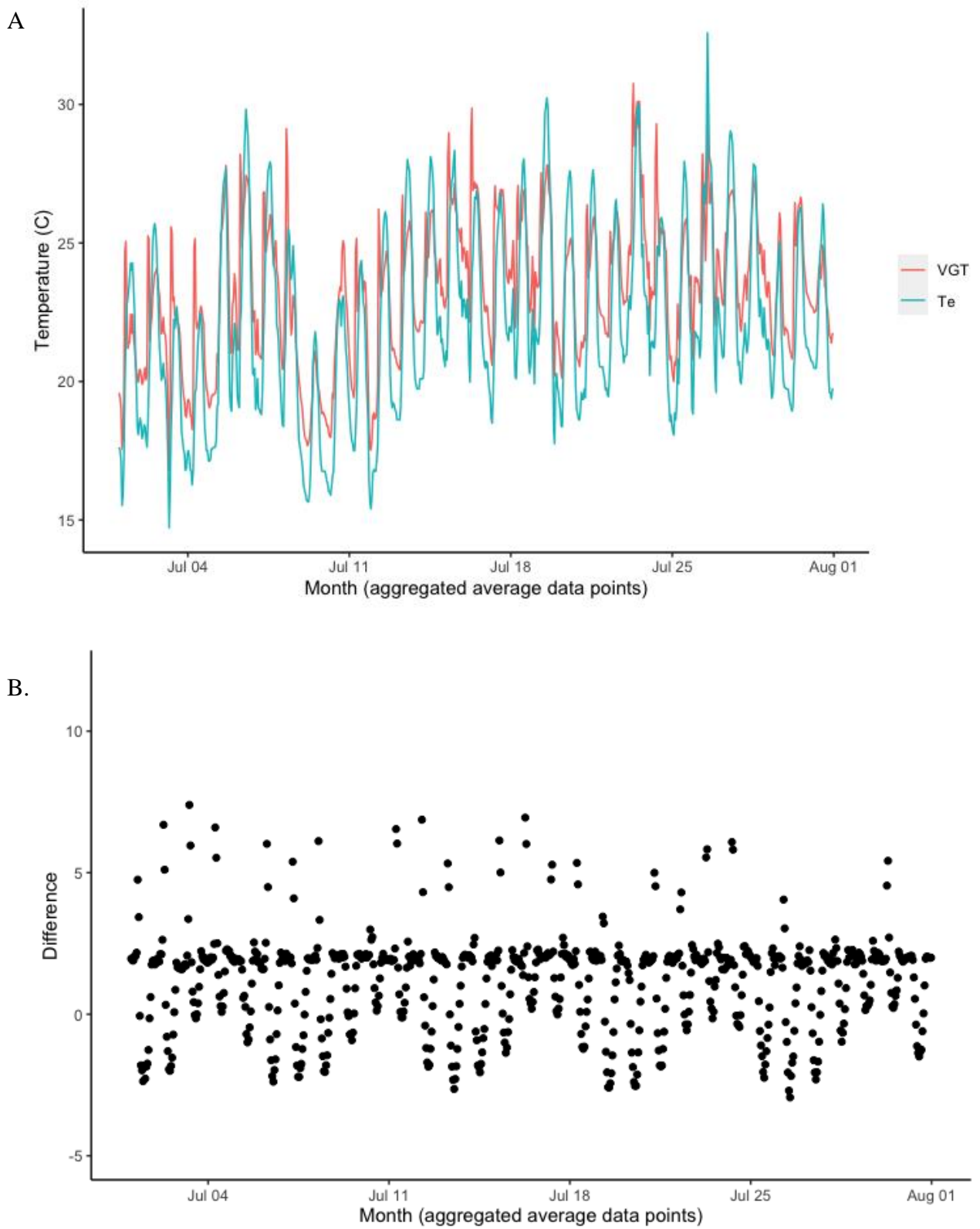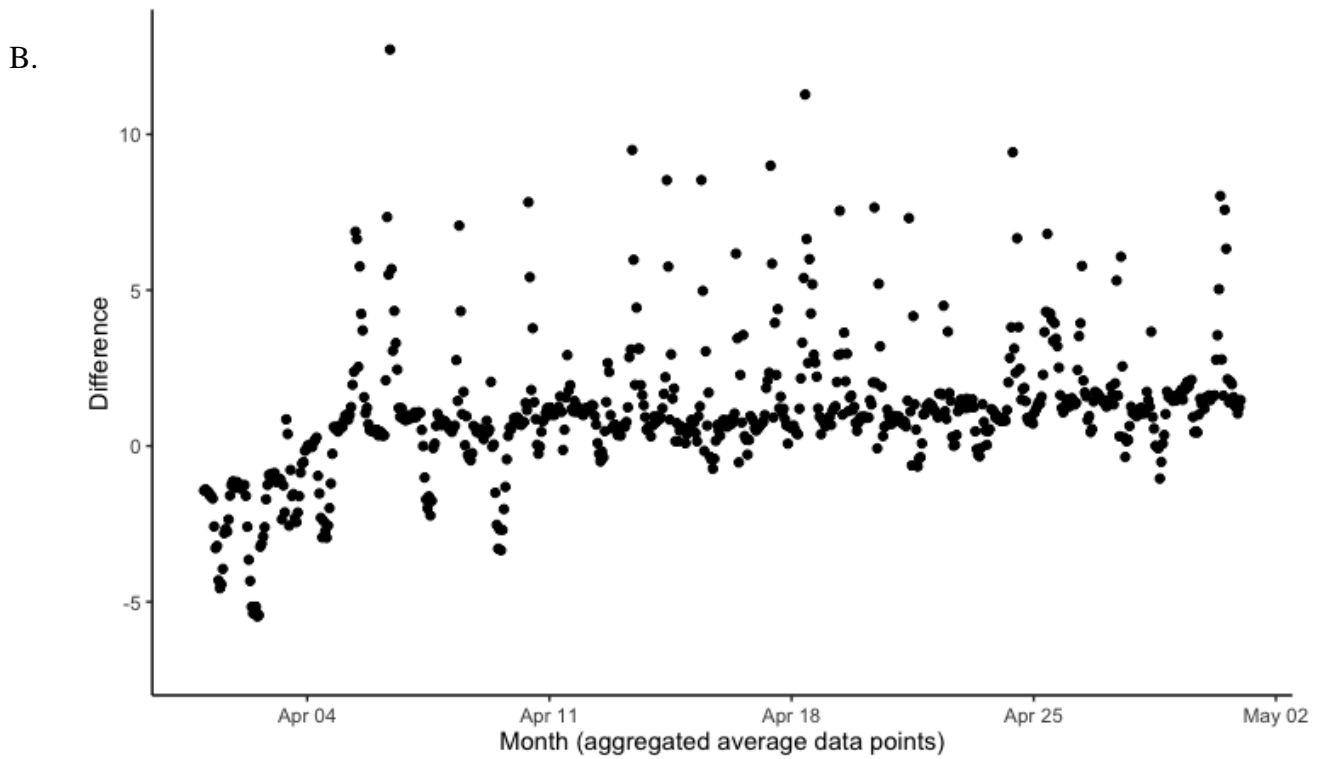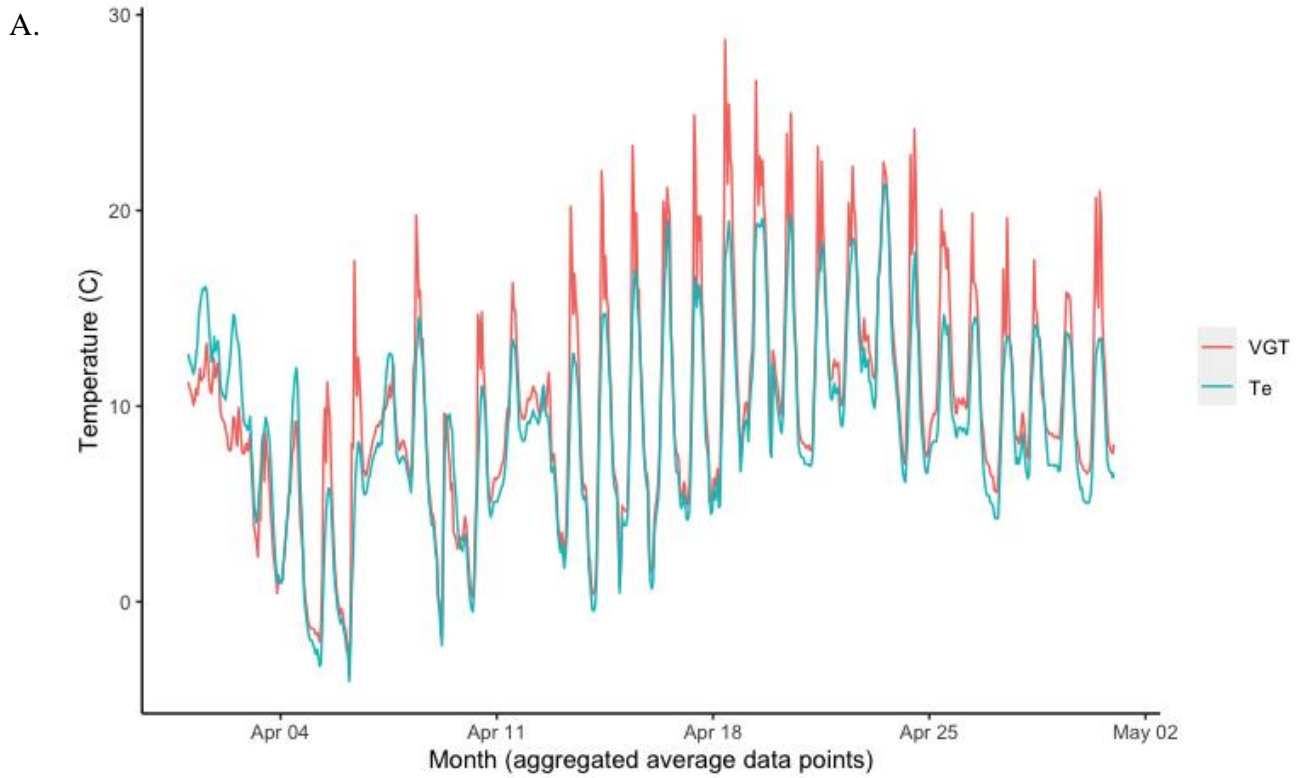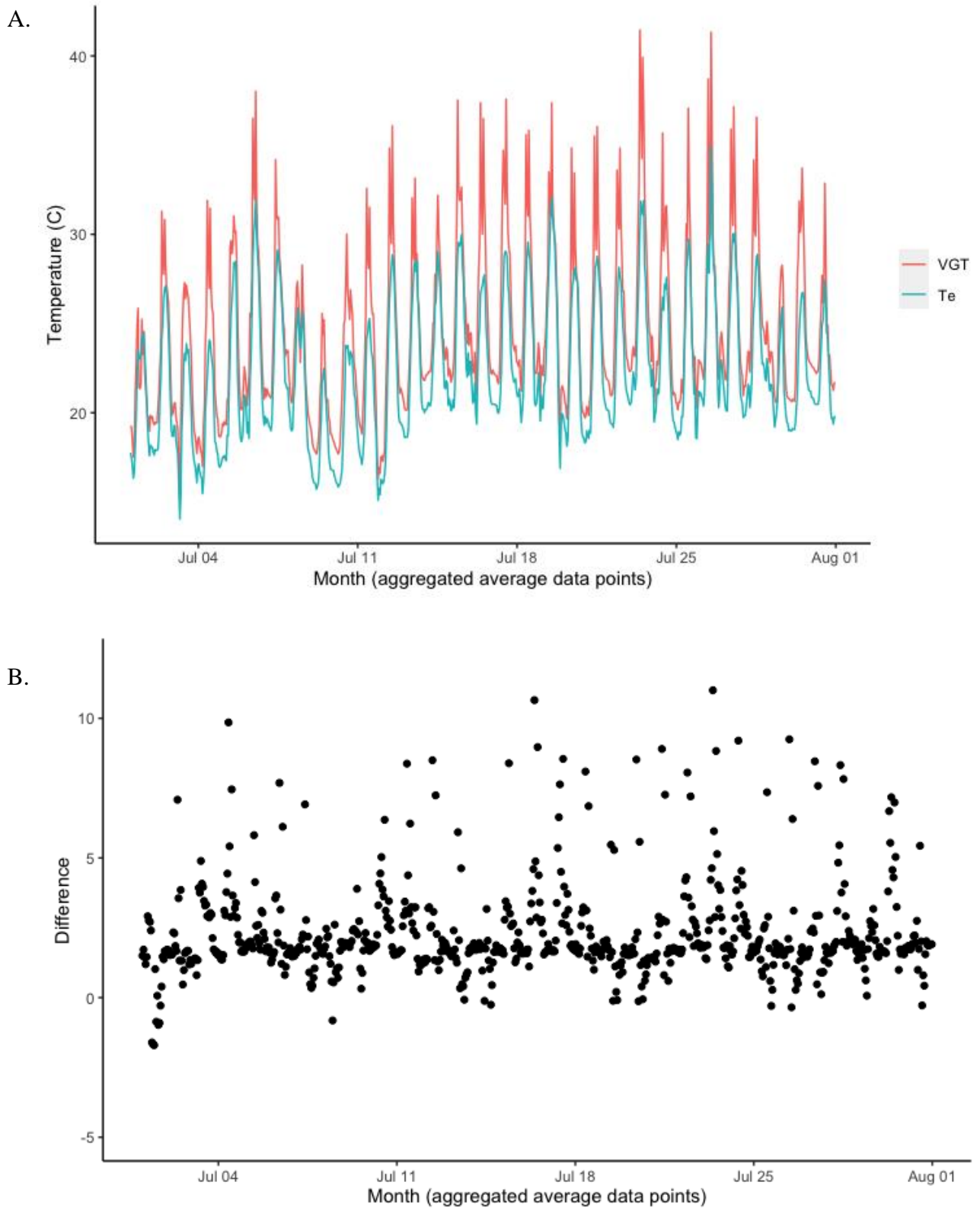
EPILOGUE

The relationship between an organism's current and future space-use and distribution in the face of climate change is an important question in ecology (Kearney et al. 2008, Kearney and Porter 2009, Porter et al. 2010). Aside from the many biotic and abiotic elements of the environment that must be considered, there have been calls to develop a species-based approach that incorporates knowledge of the organism's ability to move, its life history, body size, capacity for genetic variation and phenotypic plasticity, along with its behavior, physiology and demography (Kearney et al. 2009b, Fuller et al. 2016). While many species will face increased threats of extinction (e.g., due to the inability to travel thousands of kilometers to find suitable habitat), species that are well-adapted to live among people – such as deer – may instead benefit from the exploitation of the natural and built environment to satisfy life requisites.

The goal of this research was to validate the 127-mm Vernon globe thermometer as a surrogate for heat exchange for white-tailed deer using a model of T_e that incorporated mechanisms of heat transfer between a deer and its environment, and micrometeorological data collected from a sensor network on Fire Island. The globe was an adequate proxy; however, Fire Island is a harsh marine environment. Constant wind, extreme temperatures and salt spray create a highly corrosive environment that defies conventional water-proofing technology. Consequently, sensor malfunction or failure creates gaps in data streams which requires remediation. In order to accurately reconstruct the missing data, a method that can predict missing values while simultaneously addressing the temporal and spatial autocorrelation among and between sensors in the network will be necessary.

Given the advent of technology that can remotely collect spatio-temporal data from a variety of sensors, there is a growing need for analytical tools to process large amounts of data

and to account for corrupted or missing observations that are inevitable across networks deployed in harsh and/or unpredictable environments (Büntgen et al. 2017, Cheng and Lu 2017). Spatio-temporal modeling has emerged as a way to categorize current space-use by an organism, understand variations in behavior and also predict future patterns, especially in locations where data was unobserved (Massé and Côté 2013, Long et al. 2014, Bakar and Kokic 2017).

The R package, spTimer, for Spatio-Temporal Bayesian Modeling, fits, spatially predicts, and temporally forecasts large amounts of space-time data. spTimer contains numerous functions to analyze, extract, modify and visualize results, obtain credible intervals for model parameters and validate predicted observations with values obtained from independent data (Sahu and Bakar 2012, 2015, 2018). Future research will involve developing an autoregressive, spatio-temporal model using spTimer that can be fit using hourly aggregated data from the stations, so that the model can generate spatio-temporal predictions of Vernon globe temperature. These predictions will be validated using an independent, holdout sensor (the Base Station) and utilized in constructing a map of the daily thermal environment of deer from ocean to bay. The map can be used to identify suitable locations for deer to meet their biological needs as well as act as a risk map to highlight areas where deer-vehicle collisions, tick presence and damage to landscaping might be prevalent. This will further be incorporated into resource selection functions and supplemented with activity data from deer equipped with Very High Frequency/Global Positioning System satellite and radio-telemetry technology in order to develop hypotheses regarding behavioral responses and space-use by deer under future climate warming scenarios between the built and natural environments of Fire Island.

REFERENCES

Arnold, W., C. Beiglböck, M. Burmester, M. Guschlbauer, A. Lengauer, B. Schröder, M. Wilkens, and G. Breves. 2015. Contrary seasonal changes of rates of nutrient uptake, organ mass, and voluntary food intake in red deer (*Cervus elaphus*). American Journal of Physiology - Regulatory, Integrative and Comparative Physiology 309:R277-285.

Art, H. W. 1976. Ecological studies of the Sunken Forest, Fire Island National Seashore, New York (Vol. 7). National Park Service.

Bakar, K. S., and P. Kokic. 2017. Bayesian gaussian models for point referenced spatial and spatio-temporal data. Journal of Statistical Research 51:17-40.

Bakken, G. S., and D. M. Gates. 1975. Heat-transfer analysis of animals: some implications for field ecology, physiology, and evolution. Pages 255-290 *in* D. M. Gates and R. B. Schmerl, editors. Perspectives of biophysical ecology. Springer-Verlag, New York, New York, USA.

Bakken, G. S. 1976. A heat transfer analysis of animals: unifying concepts and the application of metabolism chamber data to field ecology. Journal of Theoretical Biology 60:337-384.

Bakken, G. S., W. R. Santee, and D. J. Erskine. 1985. Operative and standard operative temperature: tools for thermal energetic studies. American Zoologist 25:933-943.

Bakken, G. S. 1992. Measurement and application of operative and standard operative temperatures in ecology. American Zoologist 32:194-216.

Bartelt, P. E., R. W. Klaver, and W. P. Porter. 2010. Modeling amphibian energetics, habitat suitability, and movements of western toads, *Anaxyrus* (=*Bufo*) *boreas*, across present and future landscapes. Ecological Modelling 221:2675-2686.

Beaver, J. M., B. E. Olson, and J. M. Wraith. 1996. A simple index of standard operative

    temperature for mule deer and cattle in winter. Journal of Thermal Biology 21:345-352.

Belovsky, G. E. 1981. Optimal activity times and habitat choice of moose. Oecologica 48:

    22-30.

Boldrini, J. L., M. P. Viana, S. F. dos Reis, and B. Henning. 2018. A mathematical model for

    thermoregulation in endotherms including heat transport by blood flow and thermal

    feedback control mechanisms: changes in coat, metabolic rate, blood fluxes, ventilation

    and sweating rates. Letters in Biomathematics 5:129-173.

Brownstein, J. S., T. R. Holford, and D. Fish. 2005. Effect of climate change on Lyme Disease

    risk in North America. EcoHealth 2:38-46.

Bunnell, F. L., K. L. Parker, L. L. Kremsater, and F. W. Hovey. 1986. Thermoregulation and

    thermal cover of deer and elk on Vancouver Island: a problem analysis. The Ministry of

    Environment and Parks and the Ministry of Forests and Lands, Victoria, British

    Columbia, Canada.

Büntgen, U., L. Greuter, K. Bollmann, H. Jenny, A. Liebhold, J. D. Galván, N. C. Stenseth, C.

    Andrew, and A. Mysterud. 2017. Elevational range shifts in four mountain ungulate

    species from the Swiss Alps. Ecosphere 8:e01761.

Campbell, G. S., and J. Norman. 1998. An introduction to environmental biophysics. Second

    edition. Springer Science+Business Media, New York, New York, USA.

Cheng, S., and F. Lu. 2017. A two-step method for missing spatio-temporal data reconstruction.

    ISPRS International Journal of Geo-Information 6:187.

Davis, L. B., and R. C. Birkebak. 1975. Convective energy transfer in fur. Pages 525-548 *in* D. M. Gates and R. B. Schmerl, editors. Perspectives of biophysical ecology. Springer-Verlag, New York, New York, USA.

Dawe, K. L., and S. Boutin. 2016. Climate change is the primary driver of white-tailed deer (*Odocoileus virginianus*) range expansion at the northern extent of its range; land use is secondary. Ecology and Evolution 6:6435-6451.

Duffy, D. C., S. R. Campbell, D. Clark, C. Dimotta, and S. Gurney. 1994. *Ixodes scapularis* (Acari: Ixodidae) Deer tick mesoscale populations in natural areas: effects of deer, area, and location. Journal of Medical Entomology 31:152-158.

Dusek, G. L., A. K. Wood, C. A. Sime, S. Hoekman, and J. Morgan. 2006. White-tailed deer studies in the Salish Mountains, Northwest Montana. Montana Fish, Wildlife & Parks, Wildlife Division, Helena, Montana, USA.

Dzialowski, E. M. 2005. Use of operative temperature and standard operative temperature models in thermal biology. Journal of Thermal Biology 30:317-334.

Elmore, R. D., J. M. Carroll, E. P. Tanner, T. J. Hovick, B. A. Grisham, S. D. Fuhlendorf, and S. K. Windels. 2017. Implications of the thermal environment for terrestrial wildlife management. Wildlife Society Bulletin 41:183-193.

Forrester, J. 2004. Ecological dynamics of a rare maritime *Ilex opaca* forest. Dissertation. State University of New York College of Environmental Science and Forestry, Syracuse, USA.

Forrester, J. A., D. J. Leopold and H. B. Underwood. 2006. Isolating the effects of white-tailed deer on the vegetation dynamics of a rare maritime American holly forest. American Midland Naturalist 152:135-150.

Fuller, A., D. Mitchell, S. K. Maloney, and R. S. Hetem. 2016. Towards a mechanistic understanding of the responses of large terrestrial mammals to heat and aridity associated with climate change. Climate Change Responses 3:1-19.

Hetem, R. S., S. K. Maloney, A. Fuller, L. C. R. Meyer, and D. Mitchell. 2007. Validation of a biotelemetric technique, using ambulatory miniature black globe thermometers, to quantify thermoregulatory behaviour in ungulates. Journal of Experimental Zoology Part A: Ecological Genetics and Physiology 307A:342-356.

Hetem, R. S., W. M. Strauss, L. G. Fick, S. K. Maloney, L. C. R. Meyer, M. Shobrak, A. Fuller, and D. Mitchell. 2010. Variation in the daily rhythm of body temperature of free-living Arabian oryx (*Oryx leucoryx*): does water limitation drive heterothermy? Journal of Comparative Physiology B 180:1111-1119.

Horton, R., G. Yohe, W. Easterling, R. Kates, M. Ruth, E. Sussman, A. Whelchel, D. Wolfe, and F. Lipschultz, 2014. Ch. 16: Northeast. Climate Change Impacts in the United States: The Third National Climate Assessment, J. M. Melillo, T.C. Richmond, and G. W. Yohe, Eds., U.S. Global Change Research Program, 371-395. doi:10.7930/J0SF2T3P.

Huey, R. B. 1991. Physiological consequences of habitat selection. American Naturalist 137:S91-S115.

Huey, R. B., M. R. Kearney, A. Krockenberger, J. A. Holtum, M. Jess, and S. E. Williams 2012. Predicting organismal vulnerability to climate warming: roles of behaviour, physiology and adaptation. Philosophical Transactions of the Royal Society B: Biological Sciences 367:1665-1679.

IPCC 2018: Global warming of 1.5°C. An IPCC Special Report on the impacts of global warming of 1.5°C above pre-industrial levels and related global greenhouse gas emission

pathways, in the context of strengthening the global response to the threat of climate change, sustainable development, and efforts to eradicate poverty. Intergovernmental Panel on Climate Change (IPCC).

Janour, Z. 1951. Resistance of a plate in parallel flow at low Reynolds numbers. National Advisory Committee for Aeronautics, Washington, DC, USA.

Johnston, K., and O. Schmitz. 1997. Wildlife and climate change: assessing the sensitivity of selected species to simulated doubling of atmospheric CO2. Global Change Biology 3:531-544.

Kearney, M., B. L. Phillips, C. R. Tracy, K. A. Christian, G. Betts, and W. P. Porter. 2008. Modelling species distributions without using species distributions: the cane toad in Australia under current and future climates. Ecography 31:423-434.

Kearney, M., W. P. Porter, C. Williams, S. Ritchie, and A. A. Hoffmann. 2009a. Integrating biophysical models and evolutionary theory to predict climatic impacts on species' ranges: the dengue mosquito *Aedes aegypti* in Australia. Functional Ecology 23:528-538.

Kearney, M., and W. Porter. 2009. Mechanistic niche modelling: combining physiological and spatial data to predict species' ranges. Ecology Letters 12:1-17.

Kearney, M., R. Shine, and W. P. Porter. 2009b. The potential for behavioral thermoregulation to buffer "cold-blooded" animals against climate warming. Proceedings of the National Academy of Sciences 106:3835-3840.

Kerslake, D. Mck. 1972. The stress of hot environments. Cambridge University Press, United Kingdom.

Kilheffer, C. 2018. Plant community development in storm-induced overwash fans of the Otis
    Pike Fire Island High Dune Wilderness Area, New York. Dissertation, State University
    of New York College of Environmental Science and Forestry, Syracuse, USA.

Kilheffer, C., J. Raphael, L. Ries, and H. B. Underwood. 2019. White-tailed deer movements and
    space use on Fire Island: a four-year radio-telemetry study: 2015-2016 Post-Hurricane
    Sandy Assessment. Natural Resource Report NPS/FIIS/NRR—2019/2038. National Park
    Service, Fort Collins, Colorado, USA.

Klopfer, S. D., A. Olivero, L. Sneddon, and J. Lundgren. 2002. Final report of the NPS
    vegetation mapping project at Fire Island National Seashore. United States Geological
    Survey-National Park Service Vegetation Mapping Program, Conservation Management
    Institute, Blacksburg, Virginia, USA.

Kuehn, L. A., R. A. Stubbs, and R. S. Weaver. 1970. Theory of the globe thermometer. Journal
    of Applied Physiology 29:750-757.

Kumar, L., A. K. Skidmore, and E. Knowles. 1997. Modelling topographic variation in solar
    radiation in a GIS environment. International Journal of Geographical Information
    Science 11:475-497.

Kwak, H. S., H. G. Im, and E. B. Shim. 2016. A model for allometric scaling of mammalian
    metabolism with ambient heat loss. Integrative Medicine Research 5:30–36.

Long, R. A., R. T. Bowyer, W. P. Porter, P. Mathewson, K. L. Monteith, and J. G. Kie. 2014.
    Behavior and nutritional condition buffer a large-bodied endotherm against direct and
    indirect effects of climate. Ecological Monographs 84:513-532.

Lu, C. D. 1989. Effects of heat stress on goat production. Small Ruminant Research 2:151-162.

Maia, A. S. C., R. G. da Silva, S. T. Nascimento, C. C. N. Nascimento, H. P. Pedroza, and H. G.
T. Domingos. 2014. Thermoregulatory responses of goats in hot environments.
International Journal of Biometeorology 59:1025-1033.

Maia, A. S. C., S. T. Nascimento, C. C. N. Nascimento, and K. G. Gebremedhin. 2016. Thermal
equilibrium of goats. Journal of Thermal Biology 58:43-49.

Maloney, S. K., G. Moss, T. Cartmell, and D. Mitchell. 2005. Alteration in diel activity patterns
as a thermoregulatory strategy in black wildebeest (*Connochaetes gnou*). Journal of
Comparative Physiology A 191:1055-1064.

Marchand, P. J. 2014. Life in the cold: an introduction to winter ecology. Fourth edition.
University Press of New England, Lebanon, New Hampshire, USA.

Massé, A., and S. D. Côté. 2013. Spatiotemporal variations in resources affect activity and
movement patterns of white-tailed deer (*Odocoileus virginianus*) at high density.
Canadian Journal of Zoology 91:252-263.

McCain, C. M., and S. R. B. King. 2014. Body size and activity times mediate mammalian
responses to climate change. Global Change Biology 20:1760-1769.

Melin, M., J. Matala, L. Mehtätalo, R. Tiilikainen, O. P. Tikkanen, M. Maltamo, J. Pusenius, and
P. Packalen. 2014. Moose (*Alces alces*) reacts to high summer temperatures by utilizing
thermal shelters in boreal forests – an analysis based on airborne laser scanning of the
canopy structure at moose locations. Global Change Biology 20:1115-1125.

Moen, A. N. 1973. Wildlife ecology. First edition. W.H. Freeman and Company, San Francisco,
California, USA.

Moen, A. N., and N. K. Jacobsen. 1975. Thermal exchange, physiology, and behavior of white-tailed deer. Pages 509-524 *in* D. M. Gates and R. B. Schmerl, editors. Perspectives of biophysical ecology. Springer-Verlag, New York, New York, USA.

Mysterud, A., and E. Østbye. 1999. Cover as a habitat element for temperate ungulates: effects on habitat selection and demography. Wildlife Society Bulletin 27:385-394.

National Park Service [NPS]. 2018. Fire Island National Seashore. <https://www.nps.gov/fiis/planyourvisit/fireislandwilderness.htm>. Accessed 3 March 2018.

National Park Service [NPS]. 2019a. Plants <https://www.nps.gov/fiis/learn/nature/plants.htm>. Accessed 2 Feb 2020.

National Park Service [NPS]. 2019b.White-tailed deer management plan. <https://www.nps.gov/fiis/learn/management/deer-management-plan.htm>. Accessed 22 Oct 2019.

New York State Department of Environmental Conservation. 2018a. Community deer management guide. Division of Fish and Wildlife, Albany, New York, USA.

New York State Department of Environmental Conservation. 2018b. Deer management in urban and suburban New York: A report to the New York State senate and assembly. Albany, New York, USA.

Norris, A. L., and T. H. Kunz. 2012. Effects of solar radiation on animal thermoregulation. Solar radiation. IntechOpen, Boston University, Massachusetts, USA.

O'Connor, M. P., and J. R. Spotila. 1992. Consider a spherical lizard: animals, models, and approximations. American Zoologist 32:179-193.

Panagakis, P. 2011. Black-globe temperature effect on short-term heat stress of dairy ewes housed under hot weather conditions. Small Ruminant Research 100:96-99.

Parker, K. L., and M. P. Gillingham. 1990. Estimates of critical thermal environments for mule deer. Journal of Range Management 43:73-81.

Porter, W. P., and D. M. Gates. 1969. Thermodynamic equilibria of animals with environment. Ecological Monographs 39:227-244.

Porter, W. P., and M. Kearney. 2009. Size, shape, and the thermal niche of endotherms. Proceedings of the National Academy of Sciences of the United States of America 106 Suppl 2:19666-19672.

Porter, W. P., S. Ostrowski, and J. B. Williams. 2010. Modeling animal landscapes. Physiological and Biochemical Zoology 83:705-712.

Rai, G.D. 1980. Solar energy utilization. Khanna Publishers, Delhi, India.

Rawinski, T. J. 2008. Impacts of white-tailed deer overabundance in forest ecosystems: an overview. Forest Service, U.S. Department of Agriculture, Northeastern Area State and Private Forestry, Newtown Square, Pennsylvania, USA.

Roberts, J. A., G. Coulson, A. J. Munn, and M. R. Kearney. 2016. A continent-wide analysis of the shade requirements of red and western grey kangaroos. Temperature: Multidisciplinary Biomedical Journal 3:340-353.

Sahu, S. K., and K. S. Bakar. 2012. A comparison of Bayesian models for daily ozone concentration levels. Statistical Methodology 9:144-157.

Sahu, S.K., and K. S. Bakar. 2015. spTimer: Spatio-temporal Bayesian modeling using R. Journal of Statistical Software 63:1-32.

Sahu, S. K., and K. S. Bakar. 2018. spTimer: Spatio-Temporal Bayesian Modelling: R package version 3.3.

Sarbu, I., and C. Sebarchievici. 2017. Solar radiation. Pages 13-28 *in* I. Sarbu and C. Sebarchievici, editors. Solar heating and cooling systems. Academic Press, Cambridge, Massachusetts, USA.

Saupe, E. E., M. Papes, P. A. Selden, and R. S. Vetter. 2011. Tracking a medically important spider: climate change, ecological niche modeling, and the Brown Recluse (*Loxosceles reclusa*). PLOS ONE 6:e17731.

Sharpe, P. B., and B. Van Horne. 1999. Relationships between the thermal environment and activity of Piute ground squirrels (*Spermophilus mollis*). Journal of Thermal Biology 24:265-278.

Smith, D. M. S., I. R. Noble, and G. K. Jones. 1985. A heat balance model for sheep and its use to predict shade-seeking behaviour in hot conditions. Journal of Applied Ecology 22:753-774.

Southwick, E. E., and D. M. Gates. 1975. Energetics of occupied hummingbird nests. Pages 417-430 *in* D. M. Gates and R. B. Schmerl, editors. Perspectives of biophysical ecology. Springer-Verlag, New York, New York, USA.

Thaker, M., P. R. Gupte, H. H. T. Prins, R. Slotow, and A. T. Vanak. 2019. Fine-scale tracking of ambient temperature and movement reveals shuttling behavior of elephants to water. Frontiers in Ecology and Evolution 7.

Touloukian, Y. S., S. C. Saxena, and P. Hestermans. 1975. Thermophysical properties of matter - the TPRC Data Series. Volume 11. Viscosity. Thermophysical and Electronic Properties Information Analysis Center, Lafayette, New York, USA.

Turnpenny, J. R. 1997. Potential impacts of climate change on the energy balance of UK livestock. Dissertation, University of Nottingham, United Kingdom.

Underwood, H. B. 2005. White-tailed deer ecology and management on Fire Island (Fire Island National Seashore Science Synthesis Paper). Technical Report NPS/NER/NRTR—2005/022. National Park Service, Northeast Region, Boston, Massachusetts, USA.

Walker, S. M. 2006. Influence of microclimate on white-tailed deer wintering in a residential area in the central Adirondack Mountains. Thesis, State University of New York College of Environmental Science and Forestry, Syracuse, USA.

Walsberg, G. E. 1992. Quantifying radiative heat gain in animals. American Zoologist 32:217-224.

Wenzel, H. G., and A. Forsthoff. 1989. Modification of Vernon's globe thermometer and its calibration in terms of physiological strain. Scandinavian Journal of Work, Environment & Health 15 Suppl 1:47-51.

Wiemers, D. W., T. E. Fulbright, D. B. Wester, J. A. Ortega-S, G. A. Rasmussen, D. G. Hewitt, and M. W. Hellickson. 2014. Role of thermal environment in habitat selection by male white-tailed deer during summer in Texas, USA. Wildlife Biology 20:47-56.

Winslow, C. E. A., L. P. Herrington, and A. P. Gagge. 1937. Physiological reactions of the human body to varying environmental temperatures. American Journal of Physiology-Legacy Content 120:1-22.

APPENDICES

Appendix A. Inputs to calculation of operative temperature for white-tailed deer on Fire Island

using measured and researched inputs.

The model is derived from the basic balance equation for heat transfer, where the algebraic sum
of all the heat flow mechanisms is zero:

$$P_{Sun} + P_{Rad} + P_{Cond} + P_{Conv} = 0$$

Substitute all variables outlined below and solve for operative temperature:

$$P_{Sun} - \varepsilon_D \sigma A_D T_a^4 - \frac{K_{fur} A_D (T_e - T_a)}{f_D} - \frac{K_{air} A_D (T_e - T_a)}{\delta_{BL}} = 0$$

Operative Temperature:

$$T_e = T_a + \frac{P_{Sun} - \varepsilon_D \sigma A_D T_a^4}{\frac{K_{fur} A_D}{f_D} + \frac{K_{air} A_D}{\delta_{BL}}}$$

T_e = Operative temperature (K)

T_a = Ambient temperature (K; measured by stations)

P_{Sun} = Radiant solar power (W; solar radiant energy absorption rate of deer)

$\varepsilon_D \sigma A_D T_a^4$ = Radiation (W; rate at which heat is radiated from deer)

$\frac{K_{fur} A_D}{f_D}$ = Conduction (WK^{-1}; heat transfer expression from deer through fur barrier)

$\frac{K_{air} A_D}{\delta_{BL}}$ = Convection (WK^{-1}; heat transfer expression carried from deer by air currents)

Radiant solar power (P_{Sun}):

$$P_{Sun} = P_{max} \varepsilon_D A_D \sin(\theta_{Sun}), \quad if \ \theta_{Sun} \leq 0 \ then \ P_{Sun} = 0$$

$$P_{max} = G_S (1 - \varepsilon_S) \left[1 + 0.033 \cos \left(\frac{2\pi(n-4)}{365} \right) \right]$$

$$\theta_{Sun} = \sin^{-1} [\sin(\theta_{Lat}) \sin(\theta_{Dec}) + \cos(\theta_{Lat}) \cos(\theta_{Dec}) \cos(\theta_{Hour})]$$

$$\theta_{Dec} = 23.45 \sin\left[\left(\frac{360}{365}\right)(n + 284)\right]$$

$$\theta_{Hour} = 15(t_{Hour} - 12)$$

Where: P_{Sun} = Radiant solar power (W; Rai 1980, Campbell and Norman 1998)

P_{max} = Maximum solar power density (maximum solar radiant power density incident on earth's atmosphere; Wm^{-2}; Rai 1980)

ε_D = Emissivity of surface (0.97 for deer; Belovsky 1981)

A_D = Effective thermal radiation area (1.5 m^2; Moen 1973)

θ_{Sun} = Solar elevation angle (degrees; Campbell and Norman 1998)

G_S = Solar constant (1366 Wm^{-2}; Rai 1980)

ε_S = Data site albedo (variable for each station; Campbell and Norman 1998)

n = Day of the year (1 - 365)

θ_{Lat} = Data site latitude (40.7°)

θ_{Dec} = Solar declination (degrees; Kumar et al. 1997, Sarbu and Sebarchievici 2017; note: 23.45 = earth spin axis tilt to ecliptic, 284 = days following vernal equinox)

θ_{Hour} = Hour angle (degrees; Campbell and Norman 1998)

t_{Hour} = Local time of day in hours ($0 \leq t_{Hour} < 24$)

Radiation heat loss rate (P_{Rad}):

$$P_{Rad} = -\varepsilon_D \sigma A_D T_a^4$$

Where: P_{Rad} = Rate at which heat is radiated from deer (W; Bakken 1976, 1992, Smith et al. 1985)

σ = Stefan-Boltzmann constant (5.67·10^{-8} Wm^{-2}K^{-4}; Bakken 1992)

Conductive heat loss rate (P_{Cond}):

$$P_{Cond} = -\frac{K_{fur} A_D (T_e - T_a)}{f_D}$$

Where: P_{Cond} = Rate at which heat is conducted from deer through fur barrier (W; Moen 1973, Bakken and Gates 1975, Smith et al. 1985)

K_{fur} = Thermal conductivity of fur (3.56 Wm^{-1}K^{-1}; Davis and Birkebak 1975)

f_D = Fur thickness of deer in early fall (0.017 m; Moen 1973)

Convective heat loss rate (P_{Conv}):

$$P_{Conv} = -\frac{K_{air} A_D (T_e - T_a)}{\delta_{BL}}$$

$$\delta_{BL} = 5.2 \frac{f_D}{\sqrt{Rn}}$$

$$Rn = \frac{\rho_{air} V_W f_D}{\mu_{air}} \ if \ V_W \leq 0 \ then \ Rn = 0.001$$

Where: P_{Conv} = Rate at which heat is carried from deer by air currents (W; Moen 1973, Bakken and Gates 1975, Smith et al. 1985, Bakken 1992)

K_{air} = Thermal conductivity of air (0.025 Wm^{-1}K^{-1}; Touloukian et al. 1975)

δ_{BL} = Thermal boundary layer (distance across boundary layer from deer to free stream ambient temperture; m; Janour 1951)

Rn = Reynolds number (Dimensionless number characteristic of laminar flow across deer fur; Southwick and Gates 1975)

ρ_{air} = Density of air (1.22 kg m^{-3}; Touloukian et al. 1975)

V_W = Wind speed (ms^{-1}; measured by the stations)

μ_{air} = Dynamic viscosity of air (1.80·10^{-5} kg m^{-1}s^{-1}; Touloukian et al. 1975)

Appendix B. R code for calculation of operative temperature using hourly aggregated data. Holly

Grove in April is displayed as a representation for all computations, since the only part of the

code that changes between the three stations is the name of the station, albedo and the month.

```
##############################################################
### K. Fox - Calculation of operative temperature
### September 27, 2020
###
### R Version 3.6.3
##############################################################

#Constants
Epsilon_D <- 0.97      #Surface emissivity
Sigma <- 5.67E-8       #Stefan-Boltzmann (W/(m^2*K^4))
A_D <- 1.5             #Effective area (m^2)
f_D <- 0.017               #Fur thickness (m)
theta_Lat <- 40.7*pi/180 #Data site latitude (radians)
Mu_air <- 1.80E-5      #Viscosity of air (kg/m*s)
K_air <- 0.025          #Thermal conductivity of air (W/(m*K))
G_S <- 1366            #Solar constant (W/m^2)
Rho_air <- 1.22        #Density of air (kg/m^3)
K_fur <- 3.56          #Thermal conductivity of fur (W/m*K)

library(readxl)
library(ggplot2)
library(reshape2)

setwd(". . .")

#Select station, year and month
Holly_Grove <- read_excel("Grid_predictions.xlsx", sheet =
"Holly_Grove", na = c("NA"))
Y <- format(Holly_Grove$dt, "%Y")
m <- format(Holly_Grove$dt,"%m")
d <- format(Holly_Grove$dt,"%d")
HG <- Holly_Grove[which( Y == "2016"& m == "04" & d < "31"),]
```

```
#Heat Flow Equations
n <- HG$n #Day of the year (1 - 365)
theta_Dec <- 23.45*sin((360/365)*(n+284))*pi/180  #Data Site
declination (radians)
Epsilon_S <- 0.15
T_A <- HG$ta+273
V_W <- HG$ws
t_Hour <- as.numeric(format(HG$dt,"%H"))
P_Max <- (1-Epsilon_S)*G_S*(1+0.033*cos(2*pi*(n-4)/365)) #Max
Solar Power (W/m^2)
theta_Hour <- (15*(t_Hour-12))*pi/180 #Hour Angle (radians)
theta_Sun <- asin(sin(theta_Lat)*sin(theta_Dec)+
cos(theta_Lat)*cos(theta_Dec)*cos(theta_Hour)) #Solar Elevation
Angle (Radians)
P_Sun <- P_Max*Epsilon_D*A_D*sin(theta_Sun) #Radiant Solar Power
(W)
P_Sun <- ifelse(theta_Sun>0, P_Sun,0) #P_Sun >= 0
R_n <- (Rho_air*V_W*f_D/Mu_air)
R_n <- ifelse(R_n>0, R_n,0.0001) #R_n >= 0
Delta_BL <- 5.2*f_D/(sqrt(R_n))
T_E <- T_A+((P_Sun-Epsilon_D*Sigma*A_D*T_A^4)/
((K_fur*A_D/f_D)+(K_air*A_D/Delta_BL))) #Operative Temperature
(deg, K)

#Calculate
Operative_Temp <- T_E-273  #(deg,C)
HGO <- merge(HG, Operative_Temp, by = "row.names")
names(HGO)[names(HGO) == 'y'] <- 'Operative_Temp'
HGOP <- subset(HGO, select = c(dt, bg, Operative_Temp))
names(HGOP)[names(HGOP) == 'bg'] <- 'VGT'
names(HGOP)[names(HGOP) == 'Operative_Temp'] <- 'Te'
HGOM <- melt(HGOP, id = "dt")

#Plot
ggplot(data = HGOM, aes(x = dt, y = value, color = variable)) +
geom_line() + labs(x = "Month (aggregated average data points)",
y = "Temperature (C)") + theme(plot.title = element_text(hjust =
0.5)) + theme(legend.title = element_blank()) +
theme(panel.grid.major = element_blank(), panel.grid.minor =
element_blank(),panel.background = element_blank(), axis.line =
element_line(colour = "black"))

############################ END ############################
```

CURRICULUM VITAE

Kaitlyn Fox
kfox1619@gmail.com

EDUCATION

State University of New York   Expected: Fall 2020
College of Environmental Science and Forestry
Master of Science Candidate, *Fish and Wildlife Biology and Management*
Cumulative GPA: 3.9 out of 4.0

State University of New York   Fall 2013 – Spring 2017
Stony Brook University
Bachelor of Arts, *Environmental Studies (concentration in Conservation Biology)*
Minors in *Biology* and *Geospatial Science*
Cumulative GPA: 3.8 out of 4.0
Dean's List: Fall 2013 – Spring 2017
Magna Cum Laude

RESEARCH AND WORK EXPERIENCE

Graduate Research, **SUNY ESF**   Fall 2017 – Fall 2020
- *Master's Thesis* – work in analyzing meteorological data to develop biophysical models aimed at understanding shade-seeking behavior in white-tailed deer in the built and natural environments of Fire Island, New York.

Research Assistant, SUNY SBU   Spring 2016 – Spring 2017
- *Ecology and Evolution Laboratory* – assisted in the study of invasive Zebra Mussels from the Hudson River; created algal cultures and recorded data via microscopy.
- *Primate Conservation Laboratory* – assisted in cataloging information concerning play behavior in lemurs from research logs recorded by research affiliates and graduate students.

Wildlife Rehabilitation Intern   June 2015 – August 2015
- *Sweetbriar Nature Center* – rehabilitation of wild animals such as waterfowl, birds, and small mammals.

Guide Dog Foundation Volunteer   May 2015 – August 2017
- Cared for guide dogs; worked to socialize dogs through obedience training.

TEACHING EXPERIENCE

Graduate Teaching Assistant, SUNY ESF   August 2017 - May 2019
- Courses: *General Ecology*, *Global Environment*, *Wildlife Habitats and Populations*, *Diversity of Life II*
- Taught lab courses, supervised undergraduate teaching assistants, graded reports, exams and projects and assisted students with course material.

RELEVANT COURSEWORK

Ecosystem Ecology, Primate Conservation, Conservation Biology, Mapping and Map Analysis, Geographic Information System (GIS) Design and Application I, GIS Project Management, Geospatial Science for the Coastal Zone, Wildlife Habitats and Populations, R and Reproducible Research, Winter Mammalian Ecology, Quantitative Methods and Models in R.

COMPUTER EXPERIENCE
- MS Excel, PowerPoint, Word, ArcGIS and R.